



Article

The Standard Cosmological Model: Basic Geometric and Kinematic Features

Dmitrij Nagirner ^{1,†} , and Svetlana Jorstad ^{2,‡,1,†} 

¹ Astronomy Department, St. Petersburg State University, Universitetskij Pr. 28, Petrodvorets, 198504 St. Petersburg, Russia

² Boston University, 725 Commonwealth Ave., Boston, MA, 02215, USA

* Correspondence: dinagirner@gmail.com

Abstract: We present a brief history of the construction of models of the universe, followed by calculations of quantitative characteristics of basic geometric and kinematic properties of the Standard Cosmological Model (Λ CDM). Using the Friedmann equations of uniform space, we derive equations characterizing a Λ CDM model that describes a universe corresponding to current observational data. The equations take into account the effects of radiation and ultra-relativistic neutrinos. It is shown that the universe at very early and late stages can be described to sufficient accuracy by simple formulas. Certain important moments of cosmic evolution are determined: the times when densities of the gravitational components of the universe become equal, when they contribute equally to the gravitational force, when the accelerating expansion of space begins, and several others. The dependences of different distances on redshift and the scale factor of space are derived. The distance to the sphere that expands with the speed of light (the Hubble distance), and its current and future acceleration, are found. Concepts of a horizon, second inflation, and second horizon are discussed. We consider the remote future of the universe and the opportunity, in principle, of connection with extraterrestrial civilizations.

Keywords: Standard model, first and second horizons, cosmological constant

1. Introduction

We present a brief history of the construction of cosmological models, starting with the models of A. Einstein, V. de Sitter, A. Friedmann, and J. Lemaître, and describe observational attempts to choose model parameters such as the Hubble constant and the sign of curvature of space-time. We follow the evolution of understanding of the role of the cosmological constant from its (1) introduction by Einstein to compensate for gravitational attraction, (2) later near-elimination from the theory, (3) association with some substance, and (4) recognition of this substance as the main component of the universe, currently named “dark energy,” that defines the acceleration of the expansion of space. All of these, along with ongoing technological progress, have led to the formulation of the so-called “Standard” model, which is the model that most adequately describes the existing universe.

We use the metric of Friedmann-Robertson-Walker and equations of Friedmann-Lemaître, which form the foundation of the majority of the models. We recall the definition of the “critical density” and discuss the densities of four noninteracting components of the universe: dark energy, dust matter, which includes baryonic and dark matter, radiation, and ultrarelativistic neutrinos. We derive the laws of evolution of the density of these components. Inclusion of these components allow to obtain the general solution of the equations while highlighting the case of flat space-time.

We consider the problem of the propagation of radiation in the universe from a source to the observer, a term of the geometrical horizon that arises in this case, and discuss different concepts of distances in the universe. The relationship between a time derivative of the metric distance, interpreted as the speed of expansion, and the distance itself — the Hubble-Lemaître law — and redshift is given. We explain why the cosmological redshift is not similar to the classic Doppler effect.

37 We adopt the modern parameters of the Standard model: the temperature of the cosmic microwave
38 background (CMB), the temperature of neutrino gas associated with the CMB, the Hubble constant,
39 and a share of dark energy in the total density. These parameters allow us to calculate analytically the
40 evolution of the mass density of the four components and their relative contributions to the critical
41 density, which are employed to specify relations between scale characteristics of the model and time.
42 We derive approximate formulas of these relations at the initial and remote-future epochs of expansion.
43 The evolution of a role of the components at different epochs is analysed and values of distances,
44 speeds, and accelerations as functions of redshift are calculated. We estimate a duration of the time
45 interval needed to detect a change of the redshift and apparent luminosity of a remote object with time.

46 The reasons for the existence of a second inflation and a second horizon are explained. Distances
47 to the horizons and to the place where the rate of expansion is equal to the speed of light (the Hubble
48 distance) are determined along with their speeds and accelerations. Finally, we discuss whether a
49 connection with extraterrestrial civilizations can be established in principle.

50 Based on the Standard model, the anisotropy of the cosmic microwave background, primary
51 nucleosynthesis, and the formation of large-scale structures in the universe are reproduced quite
52 accurately, as is presented in well known monographs, for example, [1–5]. Here we provide an
53 overview of the geometric and kinematic properties of the modern Standard cosmological model.

54 2. Stages of building a model

55 The path to the construction of a cosmological model, now known as the Standard model or
56 Λ CDM, was quite long. The history of this path is described in many cosmology textbooks. Here we
57 summarize the main stages of this history.

58 The intention to build a cosmological model, that is, a model of the entire universe, and not only
59 the solar system or the Galaxy, appeared as soon as A. Einstein (1917) has formulated the equations
60 of the general theory of relativity [7] (1916), which describe gravitational fields and the behavior of
61 matter in them. He applied the equations to the homogeneous and isotropic distribution of matter
62 (following the “cosmological principle”) and tried to find a stationary solution of these equations to
63 avoid problems of an origin and initial ultra-dense stages in the history of the universe. To achieve
64 this, he had to supplement the equations with the cosmological term, so-called cosmological constant,
65 or Λ parameter [7], which corresponds not to gravitational attraction, but to repulsion. The stationary
66 solution was obtained only for a closed universe and, moreover, as A. Eddington showed [8], turned
67 out to be unstable.

68 Another stationary solution was obtained by de Sitter [9] (1917) also for a closed universe, but not
69 containing matter (empty space). In this model, the passage of time at a certain point of space depends
70 on the distance to this position from the observer. The redshift of the spectrum of a remote object was
71 explained by the fact that a clock around it was running more slowly than that of an observer on the
72 Earth. According to this theory, the radius of the curvature of space that does not change with time,
73 $R = R_0$, is directly connected with the cosmological constant: $\Lambda = 3/R_0^2$. This model has prompted
74 numerous works on the study of the “de Sitter World” itself, in which properties of the symmetry of
75 space in different coordinates (see the references in [8]) were considered. In fact, these works are more
76 of a mathematical character than of cosmological insight, although they deal with some astronomical
77 aspects and observed values (speeds of galaxies, size of universe, etc.).

78 The first non-stationary solutions of the Einstein equations were obtained by a Russian
79 mathematician, fluid mechanician, and meteorologist A.A. Friedmann (1888–1925) for a matter without
80 pressure, uniformly distributed in space, first with a positive curvature [10] (1922), then with a negative
81 curvature [11] (1924). In these works he also studied cases with positive and negative values of the
82 cosmological constant.

83 The Belgian theorist G. Lemaître (1894–1966) also obtained non-stationary solutions [12] in 1927,
84 not knowing about the works by Friedmann (when reprinting the article in English, he mentioned the
85 Friedmann work [10]). Lemaître was the first who included radiation as a component of the universe

86 and analytically derived the Hubble law ahead of its observational discovery (now this law is called
87 the Hubble—Lemaître law). The idea of the Big Bang at the beginning of the expansion of the universe
88 belongs to Lemaître as well [13].

89 As for the cosmological constant, Einstein first doubted the need for its introduction [14], and
90 completely abandoned it when non-stationary solutions of the equations were obtained [15]. In 1929
91 E. Hubble, using the 100-inch Mount Wilson Telescope, discovered that the redshift of lines (translated
92 by him into speed) in spectra of weak nebulae (which he had found to be galaxies) increases with the
93 distance to them. He interpreted this as recession. This was considered as a proof of a non-stationarity
94 of the universe. However, the values of the parameters relevant to the universe remained uncertain
95 and had to be determined by observations.

96 Observers turned to clarification of the cardinal question of whether the universe is closed or
97 open, that is, what is larger: the actual mass density of matter in space, ρ , or the critical density, ρ_c ,
98 delimiting closed and open models. At that time it was believed that the universe consists of primarily
99 observable objects that radiate or absorb light, such as planets, stars, galaxies, gas, and dust that form
100 the baryonic component of the universe. Later, the dark matter was added to the baryonic component,
101 the amount of which is determined indirectly. This dark matter is manifested through the attractive
102 force of gravity: its existence explains the flat rotation curves of spiral galaxies, the compactness of rich
103 galaxy clusters, to which the virial theorem is applicable, and gravitational lensing effect. The nature
104 of this matter has not been established, but its existence explains the observations.

105 Many observational works have been devoted to answering the cardinal question. These works
106 use cosmological tests that determine the ratio $\Omega_0 = \rho/\rho_c$ (or deceleration parameter $q = \Omega_0/2$). The
107 review by [17] describes four different tests that allow one to reconcile theory and observation by
108 comparing the theoretical dependence of some quantity on cosmological redshift z with its observable
109 behavior for different values of Ω_0 . One of the tests suggests observations at different distances of a
110 “standard candle,” that is, an object (for example, a galaxy) of known intrinsic luminosity. For a long
111 time, no such object was available, since there is a variety of galaxy and quasar luminosities and the
112 evolution of luminosities is not fully understood.

113 The value of the Hubble constant H_0 is very significant, since it is used to determine the
114 critical density. The initial estimate of this constant by Hubble himself, $H_0 = 558$ km/s/Mpc,
115 was overestimated by almost ten times, because he mistook bright objects, identified later by radio
116 astronomy methods as HII regions, for stars, whereas the former are much brighter than the latter. As
117 a result, luminosities were overestimated, distances derived from them were underestimated, hence
118 the value of H_0 was overestimated, as established by A. Sandage in 1958 [18]. As time went on, the
119 Hubble constant was refined. This was the focus of a series of papers by [19]. The distance scale was
120 based on the brightest blue and red giants in galaxies, with reference to Cepheid variables. The results
121 were summarized in a review [20], although it was noted that different methods give values of H_0 that
122 differ by several times due to systematic errors of the methods. A detailed history of construction of
123 cosmological models and creation of the observational basis of cosmology is available in the book [21].

124 The cosmological term was sometimes taken into account without clarifying its meaning; more
125 often it was ignored (see the review by [22]). The physical meaning to the cosmological term was given
126 by E.B. Gliner [23]. Considering various forms of non-traditional energy-momentum tensors, he also
127 interpreted the cosmological term as such a tensor corresponding to some substance, characterizing
128 the substance as vacuum-like. Currently this substance is called “dark energy.” Its repulsive effect
129 leads to models of exponential time-dependent expansion of the universe. In the 1980s, these solutions
130 were used in the theory of cosmological inflation, which describes the earliest stages of the evolution
131 of the universe [24,25].

132 Substantial progress in determining cosmological parameters was achieved by technological
133 advances in the end of 20th century, which provided improved instruments for ground-based
134 telescopes, increased the sensitivity of receivers in different regions of the electromagnetic spectrum,
135 and made possible launches of measuring devices operating in space. As a result, observational

136 astrophysics, including cosmology, has become a multi-wavelength science. The decisive step towards
 137 the most adequate model of the real universe was made by two groups that used as a standard candle
 138 supernovae (SN) of type Ia, since the light curves of such SNs reliably determine their luminosity.
 139 Group one ([26]) using 10 SNs and group two ([27]) using 42 SNs have found that the main contribution
 140 to the critical density corresponds to the cosmological constant Λ . Both papers mentioned above
 141 describe the history of employing SN of this type as a standard candle. For example, this was done by
 142 [19], who used 16 SNs from the Coma Berenices and Virgo clusters to construct a Hubble diagram,
 143 with the calibration based on two close supernovae, 1937c in the galaxy IC4182 and 1954a in NGC4214.
 144 However, this was insufficient to make accurate conclusions.

145 Subsequently, the observations were extended to the highest redshifts, up to $z=1$ and soon to
 146 $z=1.8$ [28], which confirmed the conclusion of [26,27], and rejected other interpretations (see [22]).
 147 Confirmations were obtained by other types of observations as well. Therefore, the conclusion by
 148 [26,27] that Λ plays a significant role in the cosmos became a fundamental aspect of the Standard
 149 model that best describes the universe. Although refinement of the parameters of the model continues,
 150 results of the Wilkinson Microwave Anisotropy Probe (WMAP) [29] and Planck [30,31] missions have
 151 allowed us to specify the value of H_0 with an accuracy of 10% or even 7%.

152 3. Basic equations of homogeneous cosmological models

153 In order to show the peculiarities of the Standard model we begin with a brief presentation of the
 154 general theory of homogeneous cosmological models.

155 3.1. Space-time metric

Any construction of a space-time model begins with the establishment of its metric. For
 cosmological models the metric in conventional notation has the common form: $ds^2 = c^2 dt^2 - dl^2$. It is
 convenient to determine the following alternative functions, related by the equation $cs_k^2 \chi + k sn_k^2 \chi = 1$:

$$sn_k \chi = \begin{cases} \sin \chi & \text{for } k = 1, \\ \chi & \text{for } k = 0, \\ sh \chi & \text{for } k = -1, \end{cases} \quad cs_k \chi = sn'_k \chi = \begin{cases} \cos \chi & \text{for } k = 1, \\ 1 & \text{for } k = 0, \\ ch \chi & \text{for } k = -1. \end{cases} \quad (1)$$

Then the cosmological principle, according to which everything in the universe on large scale
 at each moment is distributed uniformly and isotropically, is accepted, so that all points of space are
 equal. Everything that occurs in each of them and with respect to them is completely the same. This
 leads to the metric of space:

$$dl^2 = R^2(\eta) \left[d\chi^2 + sn_k^2 \chi d\omega^2 \right], \quad d\omega^2 = d\theta^2 + \sin^2 \theta d\varphi^2, \quad (2)$$

156 where η and χ are dimensionless (conformal) time and spatial coordinates, with $k=1,0,-1$
 157 corresponding to closed, flat, and open space, respectively, $R(\eta)$ is the radius of curvature, and
 158 $d\omega^2$ is the metric on a sphere of unit radius, with angular coordinates θ and φ . The curvature, k/R^2 , is
 159 constant at every moment over entire space. The only point of space that needs to be specified is the
 160 location of the observer (humanity), and the reference time, which is the current epoch.

Let us fix a moment t and the corresponding conformal time η and draw a ray with the beginning
 at the position of the observer O, with direction determined by spherical angles $\theta = \theta_0$, $\varphi = \varphi_0$. There
 is a point on the sphere with a radius of unity which corresponds to this ray such that the distance
 $d\omega = 0$. Let us choose a point P on the ray at distance l from point O and with a spatial coordinate
 χ , and draw a sphere, all points of which are at a distance l from point O, so that it passes through
 the selected point P. Note that in the general case (if $k \neq 0$) the point O is not the center of the sphere
 (let us call it a quasi-center), the radius of the sphere, r , is not equal to l , and the ray is not a straight
 line. (In analogy, the radius of a parallel on the Earth's surface is not equal to the distance between the

parallel and pole; the latter is not the center of the parallel, and a ray goes along the meridian, which is not a straight line.) The connection of l and r with a radius of curvature is expressed by the following equations:

$$l = R(\eta)\chi, \quad r = R(\eta) \operatorname{sn}_k \chi, \quad (3)$$

161 wherein $l > r$ at $k = 1$, $l < r$ at $k = -1$, and $l = r$ at $k = 0$.

The adoption of a space metric defines all geometric properties of space. For example, the volume of space in a sphere whose points lay on the distance $l = R(\eta)\chi$ from O ($\chi = 0$). A radius of the sphere is $R(\eta) \operatorname{sn}_k(\chi_0)$ for $k \neq 0$ is equal to

$$V(\eta, \chi) = R^3(\eta)4\pi \int_0^{\chi_0} \operatorname{sn}_k^2 \chi d\chi = R^3(\eta)2\pi \left| \chi_0 - \frac{1}{2} \operatorname{sn}_k(2\chi_0) \right|. \quad (4)$$

162 For $k = 1$ the total volume of the space, $2\pi^2 R^3(\eta)$, is finite, since $\chi \leq \pi$. For $k = 0$, it is formally
163 necessary to replace $\operatorname{sn}_k(2\chi_0)$ by its Taylor series representation up to the χ_0^3 term.

The conformal time η is connected with the usual time, which is fixed by the value of the density, by the equality $c dt = R(\eta) d\eta$. In these variables, the metric takes the form of the Friedmann-Robertson-Walker metric:

$$ds^2 = R^2(\eta) \left[d\eta^2 - d\chi^2 - \operatorname{sn}_k^2 \chi d\omega^2 \right]. \quad (5)$$

164 3.2. The Friedmann Equations

165 From the equations of the Einstein theory of gravitation (GR) with the metric (3), two equations
166 for the radius of curvature can be derived, known as the Friedmann equations:

$$\ddot{R} = -\frac{4\pi G}{3} \left(\rho + 3\frac{P}{c^2} \right) R + \frac{\Lambda c^2}{3} R, \quad (6)$$

$$\dot{R}^2 = \frac{8\pi G}{3} \rho R^2 + \frac{\Lambda c^2}{3} R^2 - kc^2. \quad (7)$$

167 Here ρ is the total mass density of matter and radiation, P is their total pressure, and Λ is the
168 cosmological constant.

The terms with the cosmological constant in Eqs. (6)–(7) can be appended to the first term in each expression, which allows us to determine the total mass density and pressure, as well as the gravitational mass density:

$$\rho_t = \rho + \rho_\Lambda, \quad P_t = P + P_\Lambda, \quad \rho_g = \rho_t + 3\frac{P_t}{c^2}. \quad (8)$$

To satisfy these relations, it is necessary to determine the density and pressure corresponding to the cosmological term as follows:

$$\rho_\Lambda = \frac{\Lambda c^2}{8\pi G}, \quad P_\Lambda = -\frac{\Lambda c^4}{8\pi G}. \quad (9)$$

169 It is negative pressure that produces repulsion.

170 Then the equations can be written in shorter form:

$$\ddot{R} = -\frac{4\pi G}{3} \rho_g R, \quad (10)$$

$$\dot{R}^2 = \frac{8\pi G}{3} \rho_t R^2 - kc^2, \quad (11)$$

or, for a scale factor $a = \frac{R}{R_0} = \frac{1}{1+z}$,

$$\ddot{a} = -\frac{4\pi G}{3}\rho_g a, \quad \dot{a}^2 = \frac{8\pi G}{3}\rho_t a^2 - \frac{kc^2}{R_0^2}. \quad (12)$$

171 The past corresponds to the values $a < 1$; at the current epoch $t = t_0$, $R = R_0$, $a = 1$, and redshift
172 $z = 0$; and for the future $a > 1$, $-1 < z < 0$. According to its definition, the scale factor is tied to the
173 current epoch.

For compatibility of the equations, an additional condition is required:

$$\dot{\rho}_t = -3\left(\rho_t + \frac{P_t}{c^2}\right)H, \quad (13)$$

where the new variable, $H = \frac{\dot{R}}{R}$, like the radius of curvature, depends only on time. We call it the
"Hubble parameter." Its current value, H_0 , is the Hubble constant. The relation (13) can be interpreted
as the condition of adiabatic expansion of space along with its contents, since it implies that the
differential of the total energy in volume V satisfies

$$d(c^2\rho_t V) = -P_t dV. \quad (14)$$

Equation (10) also yields an equation that the Hubble parameter obeys:

$$\dot{H} = -H^2 - \frac{4\pi G}{3}\rho_g. \quad (15)$$

174 3.3. Non-interacting components

175 After the annihilation of electron-positron pairs, the composition of the universe became simpler,
176 and since then its components have been the non-relativistic matter (including baryons and dark
177 matter), radiation, neutrinos, and so-called dark energy (formerly called the vacuum), whose density
178 and pressure are given by formulas (9). Of course, at high temperatures the matter was relativistic, but
179 then its abundance was small. Similarly, due to the finiteness of the mass, at low temperatures neutrinos
180 transformed from ultrarelativistic to relativistic (moderately or weakly) or even non-relativistic, but by
181 then their mass fraction was small and difference of their masses from zero do not affect evolution
182 of the universe [32]. Therefore, we assume that during the entire evolution of the universe over the
183 period under consideration, the matter has not exerted pressure. This means that the matter has been
184 non-relativistic (dust-like), while all kinds of neutrinos can be treated as ultra-relativistic.

185 We can assume that during this period the four components did not interact with each other. Dark
186 energy in general does not interact with anything, while the interaction of cosmological neutrinos with
187 matter essentially ceased before the annihilation epoch. Radiation interacted with matter, namely, free
188 electrons and photons interacted until the end of the recombination epoch. However, after annihilation
189 and establishment of equilibrium distributions, Compton (Thompson) scattering changes significantly
190 neither the number of photons and electrons nor their energies. Therefore, the evolution of the
191 components took place independently thereafter.

In view of the foregoing, the equations of state of the four indicated components: the dust matter
(d), the radiation (r), neutrinos (ν), and dark energy (Λ) are written in the form

$$P_d = 0, \quad P_r = \frac{c^2}{3}\rho_r, \quad P_\nu = \frac{c^2}{3}\rho_\nu, \quad P_\Lambda = -c^2\rho_\Lambda. \quad (16)$$

The condition (13) is fulfilled for each non-interacting component separately:

$$\dot{\rho}_d = -3\rho_d H, \quad \dot{\rho}_r = -4\rho_r H, \quad \dot{\rho}_\nu = -4\rho_\nu H, \quad \dot{\rho}_\Lambda = 0. \quad (17)$$

The equations are easily integrated, which provides the evolution of the densities of the components:

$$\rho_d = \frac{\rho_d^0 R_0^3}{R^3} = \frac{\rho_d^0}{a^3}, \quad \rho_r = \frac{\rho_r^0 R_0^4}{R^4} = \frac{\rho_r^0}{a^4}, \quad \rho_\nu = \frac{\rho_\nu^0 R_0^4}{R^4} = \frac{\rho_\nu^0}{a^4}, \quad \rho_\Lambda = \rho_\Lambda^0. \quad (18)$$

192 Here, as above, the index 0 means belonging to the current epoch.

193 3.4. Critical parameters

In theory, the critical density, which plays an important role, and the fraction of all components in it are defined as:

$$\rho_c = \frac{3H^2}{8\pi G}, \quad \rho_t - \rho_c = k \frac{3c^2}{8\pi GR^2}, \quad \Omega_t = \frac{\rho_t}{\rho_c}, \quad \Omega_t - 1 = k \frac{c^2}{R^2}. \quad (19)$$

The sign of differences $\rho_t - \rho_c$ and $\Omega_t - 1$ coincides with the sign of k . If $\rho_t - \rho_c = 0$ then $\Omega_t - 1 = 0$ and $k = 0$. The shares of individual components are also determined:

$$\Omega_d = \frac{\rho_d}{\rho_c}, \quad \Omega_r = \frac{\rho_r}{\rho_c}, \quad \Omega_\nu = \frac{\rho_\nu}{\rho_c}, \quad \Omega_\Lambda = \frac{\rho_\Lambda}{\rho_c}, \quad \Omega_t = \Omega_d + \Omega_r + \Omega_\Lambda. \quad (20)$$

The densities of the components are expressed in terms of the current critical density and their current shares in it:

$$\rho_d = \rho_c^0 \frac{\Omega_d^0}{a^3}, \quad \rho_r = \rho_c^0 \frac{\Omega_r^0}{a^4}, \quad \rho_\nu = \rho_c^0 \frac{\Omega_\nu^0}{a^4}, \quad \rho_\Lambda = \rho_c^0 \Omega_\Lambda^0, \quad \rho_c^0 = \frac{3H_0^2}{8\pi G}. \quad (21)$$

Since radiation and neutrinos evolve in the same way, one can introduce their common density and pressure:

$$\rho_{rv} = \rho_r + \rho_\nu = \rho_c^0 \frac{\Omega_{rv}^0}{a^4}, \quad P_{rv} = P_r + P_\nu = \frac{c^2}{3} \rho_{rv}, \quad \Omega_{rv} = \frac{\rho_{rv}}{\rho_c}. \quad (22)$$

Using introduced quantities, the second equation for the scale factor (12) is rewritten in the form:

$$H = \frac{\dot{a}}{a} = \frac{H_0}{a^2} \sqrt{\Omega_{rv}^0 + \Omega_d^0 a + \Omega_\Lambda^0 a^4 - \frac{kc^2}{R_0^2 H_0^2} a^2}. \quad (23)$$

194 The first equation has already been taken into account in formulas (21). A solution of equation (23)
195 represents an implicit dependency of the scaling factor on time. At the right hand of (23) under the
196 square-root there is a fourth-order polynomial with respect to a . This form of the solution was obtained
197 by Lemaître [12]. Friedmann's solutions [10,11] did not take into account the radiation, so that the
198 polynomial under the root was of the third order.

199 3.5. Radiation, horizon, and distances

200 The equation of motion of a photon along the ray $\theta = \theta_0$, $\varphi = \varphi_0$ toward us follows from the
201 equality $ds = 0$, and connects its spatial and temporal coordinates: $\chi = \eta_0 - \eta$. At the instant of
202 emission $\chi_e = \eta_0 - \eta_e$. Since $\eta_e \geq 0$, it follows that $\chi_e \leq \eta_0$. The equality $\chi_e = \eta_0$ defines a spherical
203 horizon; photons left this horizon at the initial moment. For $\chi_e > \eta_0$ a photon, even released in our
204 direction, still has not managed to reach us. This is a geometric horizon. There is also a physical
205 horizon, which is the sphere of the last scattering during cosmological recombination. One can look
206 beyond it: the theory of nucleosynthesis and the interpretation of distortions of the cosmic microwave
207 background or relic radiation allow us to do so. However, it is impossible in principle to look behind
208 the geometric horizon.

209 In cosmology, several concepts of distances can be introduced. McCrea [33] was the first to pay
210 attention to this, and gave definitions of the distances.

- 211 1. A metric distance l , which is the distance along the line of sight drawn from the observer with
212 fixed angles (see formula (3)).
- 213 Other distances are determined by a common principle: the expression for any value in an
214 expanding and, generally speaking, non-planar space, is written down, and then this expression
215 is equated to the expression that would be true for the usual Euclidean space at a given distance.
216 The distance is named according to the quantity for which formulas are written. Usually, the
217 following distances from the observer are used (we define these at an arbitrary epoch, $t = t(\eta)$,
218 but for the selected point where we, humanity, are located).
- 219 2. For the angular size. For the angular size. Let two signals issue at moment $t_{\text{source}} = t(\eta - \chi)$ from
220 two points located from the observer at equal distance corresponding to the spatial coordinate
221 χ , and separated by an infinitesimally small angular distance, $d\omega$. Let these signals arrive
222 at the observer at moment $t = t(\eta)$. Then the linear distance between the points is $dD_{\text{ad}} =$
223 $R(\eta - \chi) \text{sn}_k(\chi) d\omega = l_{\text{ad}} d\omega$. This implies that the distance $l_{\text{ad}} = R(\eta - \chi) \text{sn}_k \chi$ is the radius of
224 the sphere with quasi-center coinciding with the observer. The moment $\eta - \chi$ corresponds to
225 points for which this distance is determined. The distance becomes zero for $\chi = 0$ (at the point of
226 the observer, as one might expect) and when $\chi = \eta$ (on the horizon). At some point the angular
227 size has a minimum value. This means that the angular size of objects with the same linear size
228 decreases in the beginning as the object recedes from the observer, and after passing the distance
229 at which the angular size reaches its minimum value, it increases. This is due to the fact that in
230 remote areas that correspond to earlier stages of expansion, the universe had a smaller scale, so
231 that the lines of sight were closer to each other. Similarly, when a rail of a certain size is crossing
232 from one pole of the Earth to another, first its angular size decreases, and then increases, since
233 the meridians converge approaching the poles.
- 234 3. For the parallax $l_{\text{pl}} = R(\eta) \text{sn}_k \chi$, which is the radius of the sphere, but rather with a quasicenter
235 at the point to which the distance is measured, and at the time of the measurement.
- 236 4. For the number of photons received by the observer from the source, taking into account the
237 difference in passage of time at the source and the observer, $l_{\text{nb}} = l_{\text{pl}} \sqrt{R(\eta)/R(\eta - \chi)}$.
5. For the apparent bolometric luminosity (called also photometric distance) $l_{\text{bb}} = l_{\text{pl}} R(\eta)/R(\eta - \chi)$,
where in addition to the difference in the passage of time, the loss of radiative energy due to
redshift is taken into account. If the luminosity of an object located at the position corresponding
to the radius of curvature $R(\eta)$ is equal to L_{O} , then the observed luminosity according to the
definition of distance derived from the bolometric brightness is equal to:

$$L_{\text{bb}} = \frac{L_{\text{O}}}{4\pi l_{\text{bb}}^2}. \quad (24)$$

To obtain the current values of these distances, it is necessary to substitute $\eta = \eta_0$, and $R(\eta_0) = R_0$.
Modern distances are related as follows:

$$l_{\text{bb}}^0 = l_{\text{nb}}^0 \sqrt{1+z} = l_{\text{pl}}^0 (1+z) = l_{\text{ad}}^0 (1+z)^2 = R_0 \text{sn}_k(\chi) (1+z). \quad (25)$$

238 Since $z \geq 0$, in this chain of equalities the magnitude of the distances decreases from left to right.

The velocity of change of metric distance, which is the expansion rate at an arbitrary epoch, η ,
complies with the Hubble–Lemaître law:

$$l = R(\eta)\chi, \quad v = \dot{l} = \dot{R}\chi = \frac{\dot{R}}{R}l = Hl. \quad (26)$$

239 The Hubble distance, at which the expansion velocity is equal to the speed of light, is $l_{\text{H}} = c/H$; the
240 current Hubble distance is $l_{\text{H}}^0 = c/H_0$.

The relationship between speed and redshift is more complex than that between speed and distance [34]. At the current epoch the relation is:

$$\frac{v}{c} = H_0 \int_0^z \frac{dz}{H}. \quad (27)$$

241 This connection is model dependent and admits velocities greater than the speed of light, so that the
 242 cosmological redshift is not identical to the classical Doppler effect. The reason is that a photon changes
 243 its frequency not only at the instant of emission from a moving source, which is taken into account by
 244 the Doppler effect, but experiences a decrease in energy at each point of its flight to the observer due
 245 to the expansion of space, which occurs according to the appropriate model. The expansion occurs
 246 identically with respect to any point considered as a center. The existence of cosmological velocities
 247 higher than the speed of light does not contradict the theory of relativity, since the mutual receding
 248 of points occurs not because of their movement, but because of the expansion of space, across the
 249 complete span of which no signals are transmitted.

250 4. The Standard model (Λ CDM)

251 4.1. Model Parameters

Modern cosmology has become a science based on observational data, which now have sufficient accuracy to construct a model that adequately describes the real universe. The most important aspect is the inference that space is very close to flat, which leads one to assume that $k = 0$. In this case the radius of curvature is infinitely large and should not appear in expressions for quantities that have physical meaning. Therefore, as is often done, we adopt for its contemporary value the Hubble distance: $R_0 = l_H^0 = c/H_0$. Then the metric (5) can be rewritten as:

$$ds^2 = (l_H^0)^2 a^2(\eta) \left[d\eta^2 - d\chi^2 - \chi^2 d\omega^2 \right]. \quad (28)$$

252 Of all the cosmological parameters, the current temperature of the radiation, which is very close
 253 to thermal (deviations from a blackbody spectrum are of order $10^{-5} \div 10^{-4}$) and called the cosmic
 254 microwave or relict background, has been determined with the greatest in cosmology accuracy: its
 255 value is $T_0 = 2.7277$ K. At an arbitrary epoch corresponding to redshift z , $T = T_0/a = T_0(1+z)$.
 256 The temperature of the neutrinos is connected to that of the radiation as $T_\nu = \sqrt[3]{4/11} T = 0.71377 T$,
 257 $T_\nu^0 = 1.9469$ K. The coefficient is obtained from the consideration that, due to the adiabatic expansion,
 258 the entropy of the total mixture of matter and radiation does not change, while during the annihilation
 259 of electron-positron pairs their entropy passes to the radiation [35]. The entropy of the neutrino gas
 260 depends only on its temperature, and does not change.

Since radiation and neutrinos are ultrarelativistic, their mass densities are proportional to the fourth power of their temperature. For radiation according to the Stefan-Boltzmann formula,

$$\rho_r^0 = \frac{a_{\text{SB}}}{c^2} T_0^4 = 4.66 \cdot 10^{-34} \text{ g/cm}^3, \quad (29)$$

where $a_{\text{SB}} = (8\pi^5 h/15c^3)(k_B/h)^4$ is called the Stefan constant. For six types of neutrinos, which are fermions rather than bosons,

$$\rho_\nu^0 = 6 \cdot \frac{7}{8} \cdot \frac{a_{\text{SB}}}{c^2} (T_\nu^0)^4 = 6.35 \cdot 10^{-34} \text{ g/cm}^3. \quad (30)$$

Together, radiation and neutrinos have a density

$$\rho_{rv}^0 = 1.10 \cdot 10^{-33} \text{ g/cm}^3. \quad (31)$$

261 The Hubble constant, according to the latest definitions, is known to within several percent: $H = 70 \pm 3$
 262 km/s/Mpc [29,31]. Here we adopt $H_0 = 70 \text{ km/s/Mpc} = 2.27 \cdot 10^{-18} \text{ 1/s}$, so that the current critical
 263 density and the Hubble distance are equal to:

$$\rho_c^0 = \frac{3H_0^2}{8\pi G} = 9.207 \cdot 10^{-30} \text{ g/cm}^3, \quad (32)$$

$$l_H^0 = \frac{c}{H_0} = 1.3215 \cdot 10^{28} \text{ cm} = 14.2 \text{ G light yrs} = 4.2828 \text{ Gpc.}$$

Current relative fractions of radiation, neutrinos, and their sum are obtained as follows:

$$\Omega_r^0 = 5.06 \cdot 10^{-5}, \quad \Omega_\nu^0 = 6.90 \cdot 10^{-5}, \quad \Omega_{rv}^0 = 1.196 \cdot 10^{-4}. \quad (33)$$

264 The main gravitational component of the mass of the universe, according to modern concepts, is
 265 dark energy; its share is estimated as 0.721 ± 0.035 [29]. Let's take the value $\Omega_\Lambda^0 = 0.72$, so that
 266 $\rho_\Lambda^0 = 6.63 \cdot 10^{-30} \text{ g/cm}^3$. Since space is flat, $\rho_t = \rho_c$ and $\Omega_t = \Omega_t^0 = 1$. The rest is a fraction of the dust,
 267 $\Omega_d^0 = 1 - \Omega_{rv}^0 - \Omega_\Lambda^0 = 0.27988 \approx 0.28$ and $\rho_d^0 = 2.577 \cdot 10^{-30} \text{ g/cm}^3$.

Cosmological densities are very low, much lower than current densities in astronomical objects. Even in interstellar space, in each cubic centimeter there is an average of ~ 1 hydrogen atom. The densities of the cosmological components correspond to the following numbers of hydrogen atoms in a cubic meter (not cm):

$$10^6 \frac{\rho_c^0}{m_H} = 5.5, \quad 10^6 \frac{\rho_\Lambda^0}{m_H} = 4.0, \quad 10^6 \frac{\rho_d^0}{m_H} = 1.5, \quad 10^6 \frac{\rho_r^0}{m_H} = 2.8 \cdot 10^{-4}, \quad 10^6 \frac{\rho_\nu^0}{m_H} = 3.8 \cdot 10^{-4}, \quad 10^6 \frac{\rho_{rv}^0}{m_H} = 6.6 \cdot 10^{-4}, \quad (34)$$

268 where $m_H = 1.67 \cdot 10^{-24} \text{ g}$. At the same time 1 cm^3 contains $n_{\text{ph}}^0 = 20.286 T_0^3 = 412$ relict photons
 269 and $6 \cdot \frac{3}{4} \cdot \frac{4}{11} n_{\text{ph}}^0 = 674$ relict neutrinos. Using the density of dark energy, the current value of the
 270 cosmological constant is determined as $\Lambda = 3 \frac{\Omega_\Lambda^0}{(l_H^0)^2} = 1.24 \cdot 10^{-56} \text{ cm}^{-2}$. Note that during inflation
 271 this density was equal to the Planck density: $\rho_\Lambda = \frac{\Lambda c^2}{8\pi G} = \rho_{\text{Pl}} = \frac{c^5}{G^2 \hbar} = 5.1593 \cdot 10^{92} \text{ g/cm}^3$, so then
 272 it was $\Lambda_{\text{Pl}} = 9.6 \cdot 10^{66} \text{ cm}^{-2}$.

273 4.2. Basic dependencies

Substituting into equation (23) $k = 0$ and dividing the variables, we obtain the relationship between the time and scale factors. Using the relationship $cdt = l_H^0 a(\eta) d\eta$, and the relationship between the time coordinate and a , we derive:

$$\int_0^a \frac{ada}{\sqrt{\Omega_{rv}^0 + \Omega_d^0 a + \Omega_\Lambda^0 a^4}} = H_0 t, \quad \int_0^a \frac{da}{\sqrt{\Omega_{rv}^0 + \Omega_d^0 a + \Omega_\Lambda^0 a^4}} = \eta. \quad (35)$$

If we introduce the notation $(\Omega_{rv}^0 + \Omega_d^0 + \Omega_\Lambda^0 = \Omega_t = 1)$,

$$H_\Lambda = H_0 \sqrt{\Omega_\Lambda^0}, \quad x_0 = \left(\frac{\Omega_\Lambda^0}{\Omega_{rv}^0} \right)^{1/4}, \quad \beta = \frac{\Omega_d^0}{(\Omega_{rv}^0)^{3/4} (\Omega_\Lambda^0)^{1/4}}, \quad \eta_* = \left(\Omega_{rv}^0 \Omega_\Lambda^0 \right)^{-1/4}, \quad (36)$$

and make the change of variable $a = x/x_0$, then the equation (23) will be transformed into

$$H = \frac{\dot{x}}{x} = H_\Lambda \frac{\sqrt{1 + \beta x + x^4}}{x^2}, \quad (37)$$

and the relations between the variables take the form

$$H_{\Lambda}t = I_1(x, \beta), \quad \eta = \eta_* I_0(x, \beta), \quad I_j(x, \beta) = \int_0^x \frac{x^j dx}{\sqrt{1 + \beta x + x^4}}. \quad (38)$$

274 The parameter of the integrals with variable upper limit is $\beta = 265.69$. The values of the constants
 275 $H_{\Lambda} = 59.397 \text{ km/s/Mpc} = 1.9249 \cdot 10^{-18} \text{ s}^{-1}$, $x_0 = 8.8088$, $\eta_* = 10.381$. The age of the universe
 276 according to the Standard model with the adopted values of the parameters is $t_0 = I_1(x_0, \beta) / H_{\Lambda} =$
 277 $4.33 \cdot 10^{17} \text{ s} = 13.722 \text{ Gyr}$.

278 The two integrals are computed numerically, although approximate representations of the
 279 integrals are possible as well. For small x , relatively simple formulas can be obtained:

$$I_0(x, \beta) \sim 2 \frac{x}{q} - \frac{1}{35} \frac{x^5}{r} \frac{1}{q^2} \left(5 + \frac{10}{q} + \frac{12}{q^2} + \frac{8}{q^3} \right) + \frac{x^9}{1716r^3 q^2} \left(99 + \frac{198}{q} + \frac{252}{q^2} + \frac{216}{q} + \frac{80}{q^4} - \frac{96}{q^5} - \frac{192}{q^6} - \frac{128}{q^7} \right), \quad (39)$$

$$I_1(x, \beta) \sim \frac{2}{3} \frac{q+1}{q^2} x^2 - \frac{x^6}{63rq^2} \left(7 + \frac{14}{q} + \frac{18}{q^2} + \frac{16}{q^3} + \frac{8}{q^4} \right) +$$

$$+ \frac{x^{10}}{2860r^3 q^2} \left(143 + \frac{286}{q} + \frac{374}{q^2} + \frac{352}{q^3} + \frac{200}{q^4} - \frac{32}{q^5} - \frac{224}{q^6} - \frac{256}{q^7} - \frac{128}{q^8} \right). \quad (40)$$

280 Here $r = \sqrt{1 + \beta x}$, $q = 1 + r$. These formulas represent the integral I_1 with a relative discrepancy of
 281 10^{-6} for $x \leq 1.9$, 10^{-5} for $x \leq 2.5$, and 10^{-4} for $x \leq 3.2$. The accuracy of the formula for I_0 is somewhat
 282 higher: the value of 10^{-6} is already achieved for $x \leq 2.1$, 10^{-5} for $x \leq 2.9$, and 10^{-4} for $x \leq 3.6$.

283 For large values of the argument, the behavior of the integrals is substantially different. The
 284 integral I_0 from $x \rightarrow \infty$ has a finite limit, while I_1 tends to infinity. Approximately, they can be
 285 represented as follows:

$$I_0(x, \beta) \sim I_0(\infty, \beta) - \frac{1}{x} \left(1 + \frac{\beta}{x^3} \right)^{1/2} F \left(1, \frac{5}{6}, \frac{4}{3}, -\frac{\beta}{x^3} \right), \quad I_1(x, \beta) \sim \ln x + S_0(\beta/x^3) + P(x_*, \beta), \quad (41)$$

$$P(x_*, \beta) = I_1(x_*, \beta) - \ln x_* - S_0(\beta/x_*^3), \quad S_0(u) = \frac{1}{3} \sum_{n=1}^{\infty} \frac{(2n-1)!!}{n(2n)!!} (-u)^n. \quad (42)$$

286 Here $F(a, b, c, x)$ is the hypergeometric function. For x_* , we can take the value of 10. For $\beta = 265.69$,
 287 the values of the integrals in the last formulas are: $I_0(\infty, \beta) = 0.42880$, $I_1(10, \beta) = 0.94380$, and
 288 $P(10, \beta) = -1.3992$. Calculations using formula (41) give the value of $I_0(x, \beta)$ with five significant
 289 digits when $x \geq 7.3$, and with (42) five significant digits of $I_1(x, \beta)$ are obtained when $x \geq 8.5$.

It should be emphasized that the scale factor a and the redshift z are tied to the current epoch, and that they change with increasing age of the universe. At the same time, the variable x is associated only with time t (through the radius of the curvature R), while the parameters β , H_{Λ} , and η_* are strictly constant. Indeed, products $M_d = \frac{4\pi}{3} \rho_d R^3 = 2.49 \cdot 10^{55} \text{ g}$ (the mass of dust matter in a sphere of radius R) and $W = 4\pi \rho_{rv} R^4 = 4.22 \cdot 10^{80} \text{ g} \cdot \text{cm}$ do not depend on time, as is also the case for the density $\rho_{\Lambda} = \rho_{\Lambda}^0$, which is proportional to the cosmological constant Λ . These values can be used to express the variable x and other parameters:

$$x = \left(\frac{4\pi \rho_{\Lambda}}{W} \right)^{1/4} R, \quad H_{\Lambda} = \sqrt{\frac{\Lambda}{3}} c, \quad \beta = \frac{3M_d}{W^{3/4} (4\pi \rho_{\Lambda})^{1/4}}, \quad \eta_* = \left(\frac{9}{16\pi} \frac{c^4}{G^2 W \rho_{\Lambda}} \right)^{1/4} = \left(\frac{9}{2} \frac{c^2}{G W \Lambda} \right)^{1/4}. \quad (43)$$

290 The variable η is directly connected with time and expressed through η_* and x .

Table 1. Epochs of equality of densities and forces.

Epoch	x	z	η	t/t_0	t Gyrs	$t_0 - t$
$\rho_d = \rho_r$	0.00159	5529	0.0151	$1.34 \cdot 10^{-6}$	$1.85 \cdot 10^{-5}$	13,7
$\rho_d = \rho_\nu$	0.00217	4057	0.0200	$2.41 \cdot 10^{-6}$	$3.31 \cdot 10^{-5}$	13.7
$\rho_d = 2\rho_r$	0.00319	2764	0.280	$4.90 \cdot 10^{-6}$	$6.72 \cdot 10^{-5}$	13.7
$\rho_d = \rho_{rv}$	0.00376	2339	0.0324	$6.64 \cdot 10^{-6}$	$9.11 \cdot 10^{-5}$	13.7
$\rho_d = 2\rho_\nu$	0.00434	2028	0.365	$8.59 \cdot 10^{-6}$	$1.72 \cdot 10^{-4}$	13.7
$\rho_d = 2\rho_{rv}$	0.00752	1169	0.0572	$2.27 \cdot 10^{-5}$	$3.11 \cdot 10^{-4}$	13.7
$\rho_{rv} = \rho_\Lambda$	1.0000	7.809	1.198	0.0488	0.669	13.0
$\rho_d = 2\rho_\Lambda$	5.1025	0.7264	2.7138	0.5261	7.219	6.5
$\rho_g = 0$	5.1050	0.7255	2.7144	0.5264	7.224	6.5
$\rho_d = \rho_\Lambda$	6.4288	0.3702	2.983	0.7043	9.66	4.06
Current	8.8088	0	3.32	1	13.7	0

291 4.3. Roles of components at different epochs

In the expressions for total mass density

$$\rho_t = \rho_c = \rho_d + \rho_{rv} + \rho_\Lambda = \rho_c^0 \Omega_\Lambda^0 \frac{1 + \beta x + x^4}{x^4} \quad (44)$$

and gravitational mass density

$$\rho_g = \rho_d + 2\rho_{rv} - 2\rho_\Lambda = \rho_c^0 \Omega_\Lambda^0 \frac{2 + \beta x - 2x^4}{x^4} \quad (45)$$

292 the mass density of dark energy is constant, while others decrease with time. Therefore, at different
293 epochs the components have played different roles.

294 At certain points in time, the densities become equal. Since the components give different
295 contributions to the gravitational mass density — the radiation gives a double positive contribution,
296 and the vacuum gives a double negative one — their effect on the gravitation is different at different
297 times. All of these moments are given in Table 1, which lists the values of the parameter x , the redshift
298 z , and the coordinate η , the fraction of the full age and the age of the universe itself at the corresponding
299 moments, as well as the time elapsed from these moments to the present epoch. The gravitational mass
300 density becomes zero at a value of x determined by the equation $x^4 - (\beta/2)x - 1 = 0$. Moments when
301 $\rho_d = \rho_\Lambda$ and when $\rho_g = 0$ almost coincide, because the radiation and neutrino densities are small at
302 these moments. The moment when $\rho_{rv} = \rho_\Lambda$ corresponds to the time when x is very close to 1.

303 4.4. Distances, speeds, acceleration: past, current, and future

In the flat model, $\text{sn}_0(\chi) = \chi$, the quasicenter and real center of spheres coincide, the parallax distance and the radius of a sphere are equal to the metric distance: $l_{\text{pl}} = r = l$. In the Standard model the expressions for l/l_H^0 and the dimensionless velocity of the expansion v/c coincide as well. Indeed, at any moment:

$$\frac{v}{c} = \frac{\dot{l}}{c} = \frac{H}{c} l = \frac{l}{l_H}. \quad (46)$$

In the Standard model the metric distance from the observer in the current universe to a location with coordinate χ is given by the formula following from (26) and (38):

$$l^0 = R(\eta_0)\chi = R_0 a(\eta_0)\chi = l_H^0(\eta_0 - \eta) = l_H^0 \eta_* [I_0(x_0, \beta) - I_0(x, \beta)]. \quad (47)$$

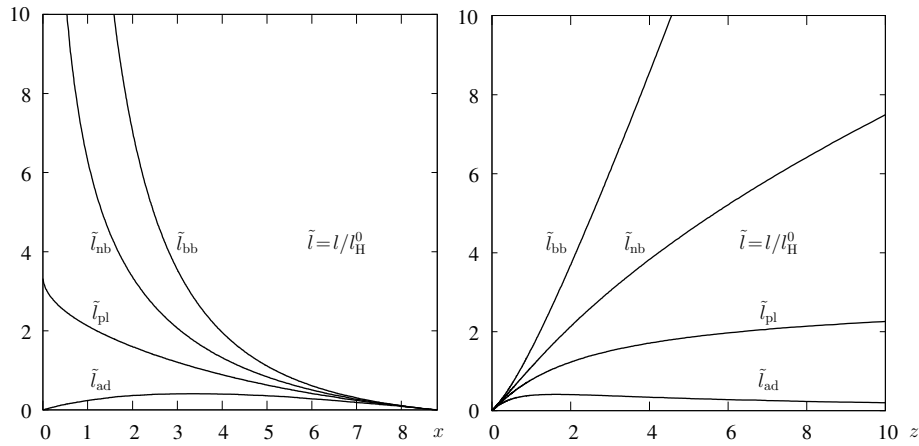


Figure 1. Distances as functions of x (left) and z (right).

Table 2. Epochs associated with the characteristic values of redshift.

x	z	η	t/t_0	t Gyrs	$t_0 - t$
0.0088000	1000	0.064629	$2.9659 \cdot 10^{-5}$	$4.0697 \cdot 10^{-4}$	13.721
0.017582	500	0.10796	$9.4743 \cdot 10^{-5}$	$1.3000 \cdot 10^{-3}$	13.720
0.087215	100	0.30606	$1.2021 \cdot 10^{-3}$	0.016494	13.705
0.17272	50	0.45696	$3.4279 \cdot 10^{-3}$	0.047036	13.675
0.80080	10	1.0642	0.034925	0.47924	13.242
0.97875	8	1.1841	0.047233	0.64811	13.074
3.3491	1.6302	2.2320	0.29360	4.0288	9.6930
3.6350	1.4233	2.3224	0.33008	4.5293	9.1925
2.2022	3	1.8084	0.15891	2.1806	0.11541

The equalities (25) can be rewritten as

$$l_{bb}^0 = l_{nb}^0 \sqrt{1+z} = l_{pl}^0 (1+z) = l_{ad}^0 (1+z)^2 = R_0 \chi (1+z) = l^0 (1+z). \quad (48)$$

In what follows, we refer mainly to current values and use dimensionless distances, measuring them in terms of the Hubble distance according to the scheme $\tilde{l} = l/l_H^0$. Therefore, all distances are expressed (as v/c in (46)) via the metric distance:

$$\tilde{l}_{pl} = \frac{v}{c} = \tilde{l} = \eta_* [I_0(x_0, \beta) - I_0(x, \beta)], \quad \tilde{l}_{ad} = \tilde{l}a, \quad \tilde{l}_{nb} = \frac{\tilde{l}}{\sqrt{a}}, \quad \tilde{l}_{bb} = \frac{\tilde{l}}{a}, \quad a = \frac{x}{x_0} = \frac{1}{1+z}. \quad (49)$$

304 Figure 1 plots dependences of distances on the variable x (left) and redshift z (right).

305 Let us consider three additional moments in time corresponding to particular events. The first
 306 event was the physical horizon (about $z = 1000$), the second was when the angular size distance had its
 307 maximum value ($z = 1.6302$), and the third was when the current metric distance equaled the Hubble
 308 distance ($z = 1.4233$). These data, and also for comparison, the moments corresponding to several
 309 characteristic values of redshift, are given in Table 2, serving as a continuation of Table 1. Table 3
 310 lists the values of the distances to the points indicated in Tables 1 and 2. The rate of change of the
 311 parallax distance coincides with v/c , since this distance corresponds to the metric distance. The
 312 rates of recession of the remaining distances are determined from their definitions by differentiation
 313 with respect to time while keeping the spatial coordinate χ fixed. The expressions for these velocities
 314 are given in Table 4.

Table 3. Distances to characteristic points of the Standard Model.

z	\tilde{l}	\tilde{l}_{ad}	\tilde{l}_{nb}	\tilde{l}_{bb}
∞	3.322	0	∞	∞
5529	3.307	$5.981 \cdot 10^{-4}$	245.9	18288
4057	3.302	$8.138 \cdot 10^{-4}$	210.4	13401
2764	3.294	$1.192 \cdot 10^{-3}$	173.2	9108
2339	3.290	$1.406 \cdot 10^{-3}$	159.2	7700
2028	3.286	$1.619 \cdot 10^{-3}$	148.0	6667
1169	3.265	$2.790 \cdot 10^{-3}$	111.7	3821
1000	3.258	$3.255 \cdot 10^{-3}$	103.1	3261
500	3.214	$6.416 \cdot 10^{-3}$	71.95	1610
100	3.016	0.02987	30.31	304.7
50	2.865	0.05619	20.46	146.1
10	2.258	0.2053	7.490	24.83
8	2.138	0.2376	6.415	19.25
7.809	2.125	0.2412	6.306	18.72
3	1.514	0.3785	3.028	6.056
1.630	1.090	0.4146	1.768	2.868
1.423	1.000	0.4126	1.557	2.423
0.7264	0.6086	0.3525	0.7996	1.051
0.7255	0.6100	0.3524	0.7987	1.049
0.3702	0.3397	0.2479	0.3977	0.4655
0	0	0	0	0

Table 4. Current velocities of recession at different distances.

Metric	ad	pl	nb	bb
$H_0 l$	$H(\eta_0 - \chi) l_{ad}$	$H_0 l_{pl}$	$\frac{3H_0 - H(\eta_0 - \chi)}{2} l_{nb}$	$[2H_0 - H(\eta_0 - \chi)] l_{bb}$

The acceleration of the cosmological expansion is determined by the first equation in (12):

$$\dot{v} = \ddot{l} = \frac{d^2}{dt^2} l_H^0 a \chi = l_H^0 \ddot{a} \chi = \frac{\ddot{a}}{a} l = -\frac{4\pi G}{3} \rho_g l = H_\Lambda^2 \frac{x^4 - \beta x/2 - 1}{x^4} l. \quad (50)$$

As already mentioned, in the gravitational mass density $\rho_g = \rho_d + 2\rho_r - 2\rho_\Lambda$ densities ρ_d and ρ_r decrease with increasing age of the universe, while $\rho_\Lambda = \rho_\Lambda^0$. Therefore, in the numerator of the last fraction in (50), the relative importance of the first term increases with time. At the present time ($x = x_0$), the gravitational mass density is negative: $\rho_g^0 = \rho_d^0 + 2\rho_r^0 - 2\rho_\Lambda^0 = -1.0677 \cdot 10^{-29} \text{ g/cm}^3$, so that the expansion occurs with an acceleration. But the acceleration at the current Hubble distance (speed equal to the speed of light) is only

$$\dot{v}_H^0 = -\frac{4\pi G}{3} \rho_g^0 l_H^0 = \frac{H_0 c}{2} (2\Omega_\Lambda^0 - \Omega_d^0 - 2\Omega_{rv}^0) = 3.94 \cdot 10^{-8} \text{ cm/s}^2 \approx 4 \text{ } \overset{\circ}{A}/\text{s}^2. \quad (51)$$

In the distant future at $t \rightarrow \infty$ ($\eta_\infty = 4.4514$)

$$a = \frac{1}{1+z} \sim \left(\frac{\Omega_d^0}{4\Omega_\Lambda^0} \right)^{1/3} e^{H_\Lambda t} = 0.46000 e^{H_\Lambda t}, \quad x \sim 4.0520 e^{H_\Lambda t}, \quad \eta \sim \eta_\infty - 2.5619 e^{-H_\Lambda t}. \quad (52)$$

315 Thus, the scale of the universe will increase exponentially, so that a second inflation will take place,
 316 which we will discuss in more detail later. However, according to (52), an exponential expansion
 317 will really begin only at $t \sim t_\Lambda = 1/H_\Lambda$. The time scale is $1/H_0 = 4.4081 \cdot 10^{17} \text{ s} = 13.969 \text{ Gyr}$,
 318 $t_\Lambda = 1/H_\Lambda = 5.1950 \cdot 10^{17} \text{ s} = 16.462 \text{ Gyr}$. We also define the distance $l_\Lambda = c/H_\Lambda = l_H^0 / \sqrt{\Omega_\Lambda^0} =$
 319 $1.5574 \cdot 10^{28} \text{ cm} = 5.0473 \text{ Gpc}$.

The speed of expansion of space at the Hubble distance is, by definition, equal to the speed of light. The velocity of recession of the Hubble distance is derived using equation (15):

$$\dot{l}_H = \frac{d}{dt} \frac{c}{H} = -\frac{c}{H^2} \dot{H} = \frac{c}{H^2} \left(H^2 + \frac{4\pi G}{3} \rho_g \right) = c \left(1 + \frac{1}{2} \frac{\rho_g}{\rho_c} \right) = \frac{c}{2} \frac{4 + 3\beta x}{1 + \beta x + x^4}. \quad (53)$$

According to this formula, at the beginning of the expansion the velocity is close to the two speeds of light, decreasing with time, and in the distant future it will approach zero. Acceleration at the Hubble distance increases with time, but remains finite:

$$\dot{v}_H = -\frac{4\pi G}{3} \rho_g l_H = -\frac{4\pi G}{3} \rho_g \frac{c}{H} = H_\Lambda c \frac{x^4 - \beta x/2 - 1}{x^2 \sqrt{1 + \beta x + x^4}} \rightarrow H_\Lambda c = 5.77 \overset{\circ}{A}/\text{s}^2. \quad (54)$$

Acceleration of the distance itself is negative:

$$\ddot{l}_H = -\frac{c}{2} \frac{H_\Lambda}{x} \frac{\beta + 16x^3 + 9\beta x^4}{(1 + \beta x + x^4)^{3/2}} \sim -c H_\Lambda \frac{9}{2} \frac{\beta}{x^3}. \quad (55)$$

320 From these formulas it is clear that the accelerations are of the same order as the product of the
 321 speed of light and the current Hubble constant, or the asymptotic value of the Hubble parameter:
 322 $cH_0 = 3 \cdot 10^{10} \cdot 2.27 \cdot 10^{-18} = 6.81 \cdot 10^{-8} \text{ cm/s}^2$, $cH_\Lambda = 5.77 \cdot 10^{-8} \text{ cm/s}^2$ (which coincides with the
 323 limit of (54)).

324 4.5. Evolution of redshift and apparent luminosity

325 As mentioned above, the scale factor a , and therefore the redshift $1+z = 1/a$ are tied to the
 326 epoch of observation. Therefore, the value of z for each sufficiently distant object should change with
 327 increasing age of the universe. Therefore, luminosities of objects should change as well. A. Sandage
 328 drew attention to this problem. He calculated the changes for the model of "dust" with different values

of Ω_d^0 ([36]). In the Appendix [37] to the paper [36], McVittie made the same calculations while adding a cosmological term. Later A.Loeb [38] (apparently independently) proposed to determine changes in the redshift z of quasars using observations of the L_α -forest with the 10-meter Keck telescope. He also transformed these changes into changes of the velocities of radiating objects. Such changes are known as the Sandage-Loeb effect.

Let us find the dependence of the change of z on the age of the universe according to the Standard model. Since for this relation the dependence of the radius of curvature on time is significant, we will write $R(t)$ without changing the notation. The redshift of lines in the spectrum of some object at a location corresponding to time $t = t(\eta)$ from the beginning of the expansion, and observed at a position corresponding to the fixed time $t_0 = t(\eta_0)$, is determined by the well known formula $1 + z = R(t_0)/R(t)$. Then z is uniquely related to time t , and equal to 0 at the observer's location, $z = 0$. For the complete definition of z , both times should be specified as arguments, i.e., $z(t, t_0)$. However, this is traditionally not done, since the epoch of t_0 is fixed; in the past $z > 0$ and in the future $-1 < z < 0$ with respect to t_0 . At this point we adopt a more detailed designation.

After some time has passed, the age of the universe has increased and the epoch to which redshifts are attached has moved to the moment $t'_0 = t(\eta'_0)$. Then an object at a given redshift has moved to time $t' = t(\eta')$ without changing its spatial coordinate χ . A connection between the moments of emission of radiation and its reception by the observer does not change in terms of the conformal coordinates, and the difference between the times of the observer and the object is preserved:

$$\chi = \eta'_0 - \eta' = \eta_0 - \eta, \quad \eta'_0 - \eta_0 = \eta' - \eta. \quad (56)$$

In particular, the infinitesimal displacements are equal as well: $d\eta_0 = d\eta$. Using the relation $cdt = R(t)d\eta$ at times t and t_0 , we obtain the relation between the differentials of time and the derivative of one with respect to the other:

$$dt_0 = \frac{R(t_0)}{c}d\eta_0 = \frac{R(t_0)}{c}d\eta = \frac{R(t_0)}{c} \frac{c}{R(t)}dt = \frac{R(t_0)}{R(t)}dt, \quad \frac{dt}{dt_0} = \frac{R(t)}{R(t_0)} = \frac{1}{1+z}. \quad (57)$$

The last relation between the passage of time of the object and the observer has already been used in section 3.5 for the transformation from a parallactic distance to a distance measured according to the flux of photons.

To detect changes of z , one must measure shifts of lines in the spectrum of a source (with the same value of the χ coordinate) at different times. The difference between the times should be much smaller than the times themselves, so increments of values can be replaced by their differentials (infinitesimally small), and it is sufficient to determine the derivatives of the variables. Using (57) we find:

$$\frac{dR(t)}{dt_0} = \frac{dR(t)}{dt} \frac{dt}{dt_0} = \dot{R}(t) \frac{R(t)}{R(t_0)}, \quad \frac{dR(t_0)}{dt_0} = \dot{R}(t_0). \quad (58)$$

From the latter we obtain ([36])

$$\frac{dz}{dt_0} = \frac{d(1+z)}{dt_0} = \frac{d}{dt_0} \frac{R(t_0)}{R(t)} = \frac{\dot{R}(t_0)}{R(t)} - \frac{R(t_0)}{R^2(t)} \dot{R}(t) \frac{R(t)}{R(t_0)} = \frac{\dot{R}(t_0)}{R(t_0)} \frac{R(t_0)}{R(t)} - \frac{\dot{R}(t)}{R(t)} = H_0(1+z) - H. \quad (59)$$

The dependence of H on z is derived if x is substituted by $x_0/(1+z)$ in (37).

A change in the redshift will result in a change in the observed luminosity of objects. The rate of change of the photometric distance in the current epoch, as follows from the equalities (24), (48) (its boundary parts $l_{bb}^0 = l^0(1+z)$) and (59), is equal (in accordance with Table 4) to:

$$\frac{dl_{bb}^0}{dt_0} = l^0(1+z) + l^0 \frac{dz}{dt_0} = H_0 l^0(1+z) + l^0 [H_0(1+z) - H] = \left(2H_0 - \frac{H}{1+z} \right) l_{bb}^0. \quad (60)$$

Then

$$\dot{L}_{bb}^0 = -2 \frac{L_O}{4\pi(l_{bb}^0)^3} \frac{dl_{bb}^0}{dt_0} = -2 \frac{L_{bb}^0}{l_{bb}^0} \frac{dl_{bb}^0}{dt_0} = -2L_{bb}^0 \left(2H_0 - \frac{H}{1+z} \right), \quad \frac{1}{H_0} \frac{d \ln L_{bb}^0}{dt_0} = -2 \left(2 - \frac{1}{1+z} \frac{H}{H_0} \right). \quad (61)$$

Figure 2 (for brevity, the derivative dz/dt_0 is denoted by \dot{z}) presents the dependencies of \dot{z}/H_0 and ratio $\dot{z}/[H_0(1+z)]$ on the (current) redshift z . First, the speed \dot{z} is positive, i.e., z increases; at $z = 2.34$ the derivative \dot{z} becomes zero. Between two zeros (at $z = 0$ and $z = 2.34$) at the point $z = 1.06$ there is a maximum equal to 0.280. The redshifts of more distant objects ($z > 2.34$) decrease; moreover, the rate of decrease grows rapidly with recession (increasing z): \dot{z}/H_0 is equal to -0.98 , -1.8 , -8.4 , -30 at $z = 4, 5, 10, 20$ respectively. For the ratio $\dot{z}/[H_0(1+z)]$, the growth is less pronounced. The derivatives \dot{z} and $\dot{z}/(1+z)$ are equal to zero at the same points, and $\dot{z}/(1+z)$ reaches the maximum at $z = 0.726$ that is smaller than the maximum of \dot{z} .

Figure 2 also presents a graph of the dimensionless derivative of the logarithm of the apparent luminosity as a function of z . When $z = 0$ this derivative equals -2 , which reflects a decrease in the solid angle of the source at the very beginning of the source's recession from the observer. At small z the rate of decrease grows slightly; at $z = 0.726$ it has maximum negative value, then decreases and becomes equal to zero at $z = 13.2$. The apparent brightness of distant objects should increase with redshift at $z > 13.2$. The effect is stronger for more distant objects, although it is unclear whether any radiating objects existed, since such redshifts correspond to times < 326 million years from the beginning of the expansion, less than a fraction 0.0238 of the current age of the universe.

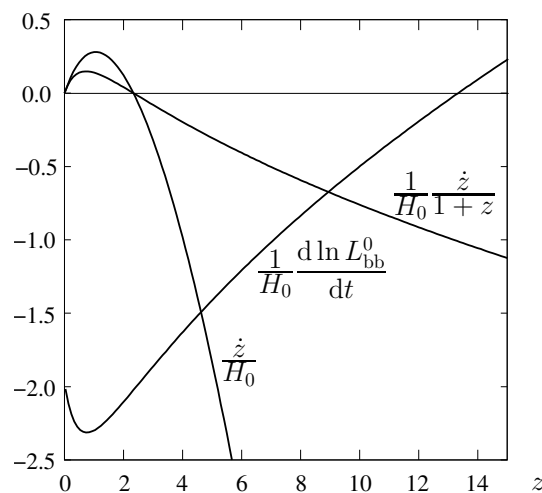


Figure 2. Changes in redshift and luminosity as a function of z .

It is most convenient to measure changes in all of these quantities when observing the L_α -forest, which corresponds to shifts of the L_α line in the spectra of distant quasars due to gas clouds located along the path to them. These clouds can have peculiar radial velocities relative to the Hubble flow that can affect observed shifts of the line. However, values of these radial components most likely do not change significantly during the time between observations if they are separated within some decades up to hundred of years. The luminosities of objects do not change as well at least in average.

Despite the importance of this effect to test the theory, any possibility of observing it with modern instruments would require a very long time interval between observations, from hundreds to thousands years, since $\lambda(t_0)/\lambda(t) = 1 + z(t, t_0)$, then $d\lambda_0/\lambda_0 = dz/(1+z)$, and

$$dt_0 = \frac{1}{H_0} \frac{dz/(1+z)}{\dot{z}/[H_0(1+z)]}. \quad (62)$$

For example, if we assume that the accuracy of measurements of a relative shift of lines is $d\lambda/\lambda = dz/(1+z) = 10^{-6}$ then for $z = 4$, as seen from Fig. 2, $\dot{z}/[H_0(1+z)] \approx -0.2$ and $dt_0 \sim 14 \cdot 10^9$.

371 $10^{-6}/0.2 = 3 \cdot 10^3$ yrs — a time interval which is insignificant on cosmological scales but longer than
 372 a human lifetime. For large z , the accuracy of measuring the position of the lines is less, so that we
 373 would need major technological progress to pursue such a method.

374 [39] estimates the possibility to detect the shift of lines due to cosmological expansion in the
 375 spectra of various objects at different wavelengths for different cosmological models when telescopes
 376 with ultra-large mirrors (40–60 m) become available, as is planned for the 2020s. It is alleged that a
 377 42-m telescope will be able to measure the shift with 4000 hour exposures separated by 40 yrs. The
 378 article also provides an overview of previous work on the question of changing redshift.

379 5. The second inflation and the second horizon

380 5.1. Visible and invisible parts of the universe

381 According to the theory of cosmological inflation, near the very beginning of the evolution of the
 382 universe, space expanded exponentially. The standard theory, as follows from (52), predicts that a
 383 positive cosmological constant causes an acceleration of space starting from a certain moment that
 384 leads to an exponential expansion, although at a much lower rate than during the first inflation. This
 385 new expansion generates a new concept: a second horizon.

The equation of motion of a photon traveling to the observer (that is, to us) is $\chi = \eta_0 - \eta$;
 therefore, the place and time of its exit are related by the equality $\chi_e = \eta_0 - \eta_e < \eta_0$. So, the equation
 of motion can be rewritten as follows: $\chi = \chi_e + \eta_e - \eta$. Therefore, the distance from the observer to
 the approaching photon is

$$l_{rs} = l_{H^0}^0 a(\eta)(\chi_e + \eta_e - \eta). \quad (63)$$

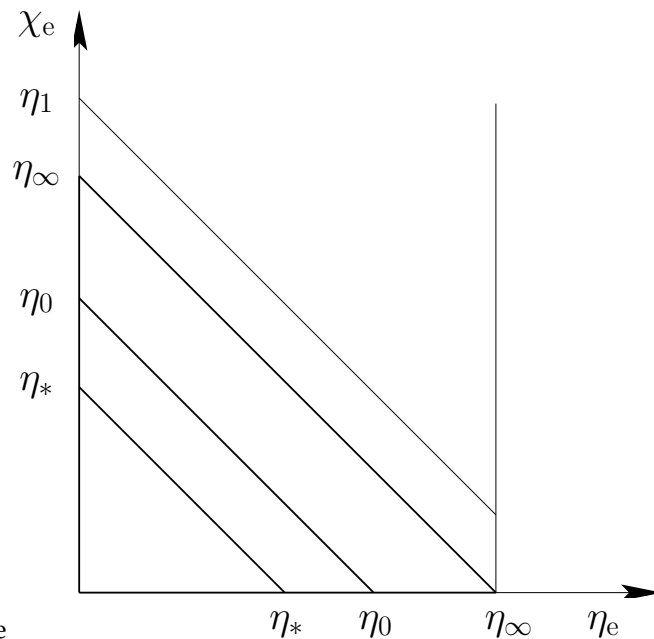
386 The parameter η is limited. For $t = \infty$, it is equal to $\eta_\infty = 4.4514$. The distance can only equal
 387 zero, $l_{rs} = 0$, if $\chi_e + \eta_e < \eta_\infty$. Then there is another limitation on the ability to observe objects in
 388 the universe: along with the first horizon there is a second one. The concept of two horizons was
 389 introduced by V. Rindler [40] and discussed in a number of papers, for example, in [41]. Here their
 390 kinematic characteristics are derived within the Standard model.

391 The first horizon is called geometric (we recall that the physical horizon is the sphere of last
 392 scattering at $z \approx 1000$), while the second horizon can be called the kinematic or dynamic horizon.
 393 Other names are also used, borrowed from the terminology of the theory of black holes. The geometric
 394 horizon is called the particle horizon, and the kinematic horizon is called the event horizon. These
 395 names were introduced by Rindler.

At an arbitrary epoch, η , the first and second horizons are determined by the equations

$$\chi_{GHor} = \eta = H_0 \int_0^a \frac{da}{a^2 H} = \eta_* I_0(x, \beta), \quad \chi_{KHor} = \eta_\infty - \eta = H_0 \int_a^\infty \frac{da}{a^2 H} = \eta_* [I_0(\infty, \beta) - I_0(x, \beta)]. \quad (64)$$

396 In Figure 3 positions of the geometric horizon are indicated on the ordinate axis. The lines
 397 corresponding to this horizon are parallel to the abscissa. They rise with time, reflecting expansion of
 398 the horizon. The second, kinematic horizon is shown by a straight line connecting the abscissa and
 399 the ordinate, which are equal to η_∞ , while its specific position corresponds to the time on the abscissa
 400 axis. The paths of photons coming toward us are represented by straight lines parallel to this straight
 401 line. Photons can start their journey from any point on the trajectory. Photons, for which $\eta_e + \chi_e < \eta_\infty$,
 402 that is, moving along straight lines lying below the straight line specified above, sooner or later will
 403 reach a place where the observer is located. For example, Figure 3 shows the paths of photons that
 404 have reached our position at time $\eta_* < \eta_0$ and at the current epoch η_0 . If $\eta_e + \chi_e > \eta_\infty$, then photons
 405 with such coordinates never reach our location. According to the equality $\eta_e + \chi_e = \eta_\infty$, it would seem
 406 that the photon still must reach the observer at least over an infinite time, but even that is impossible.



takes some additional vertical space

Figure 3. Visible and invisible parts of the universe.

407 From behind the first horizon, the radiation has not yet reached the observer. The second horizon
 408 separates the region of times and locations from which radiation cannot reach the observer, since the
 409 photons coming from there are moving away from the observer. This occurs because space expands at
 410 speeds higher than the speed of light, and these speeds increase with time. At the current time, we can
 411 see objects in the universe up to redshifts $z \approx 10$, but this corresponds to the past. We will never see
 412 objects located now at redshifts $z \geq 1.725$.

413 Indeed, if a photon is now emitted toward us from a place with coordinate χ_o , then the distance
 414 to it at moment η will be $l_{\text{ph}} = l_{\text{H}}^0 a(\eta)(\chi_o + \eta_0 - \eta)$. This distance can become equal to zero at
 415 $\eta = \chi_o + \eta_0$, and it must be the case that $\chi_o + \eta_0 < \eta_\infty$. Thus, the boundary of the coordinate χ_o
 416 for photons emitted now is $\chi_{\text{lim}}^0 = \eta_\infty - \eta_0 = 1.13$. The values of $x_{\text{lim}}^0 = 3.23$, $z_{\text{lim}}^0 = 1.725$, and
 417 $l_{\text{lim}}^0 = 4.84 \text{ Gpc} = l_{\text{KHOr}}^0$ correspond to this coordinate. The sphere of such a radius is the current second
 418 horizon. Thus, the radiation from the points now located at distances of 4.84 Gpc from us will never
 419 reach us, even in the infinitely remote future. Figure 4 shows distances l_{rs} to the photons arriving
 420 at the observer at the epoch when $\eta = 2$ (Figure 4 left), and at the current epoch (Figure 4 right). In
 421 Figure 5 these distances are given as a function of values of x for cases where the sum of the coordinates
 422 of time and location of the photon emission is equal to η_∞ (Figure 5 left) and larger than that (Figure 5
 423 right). These figures also show curves reflecting the relationship between the time η_e and the location
 424 χ_e of the photon emission.

425 Generally speaking, if a photon is emitted at a point where the expansion speed is greater than
 426 the speed of light, this does not necessarily mean that it will not reach us. Cosmological expansion
 427 occurs in the same way with respect to all points of space, and it starts after a period of inflation with a
 428 very high speed (formally infinite, according to formula (37), which defines the Big Bang), although in
 429 the beginning the expansion was slowing down. A photon emitted from far away, where the speed
 430 of expansion is large but closer than the horizon, still comes to us, because it gradually moves into
 431 layers of space expanding at a slower and slower rate. At some point its velocity toward us becomes
 432 zero, and then becomes negative, that is, it begins to approach us. However, it takes a long time for the
 433 photon to reach us. Consider, for example, a galaxy observed by us now at redshift $z = 3$: according to
 434 Table 2, it moves away from us with a speed of $H_0 l = c\tilde{l} = 1.51c$, and earlier its speed was greater. At
 435 the same time, its radiation traveled to us for 11.5 billion years, that is, we see this galaxy as it was in

/

takes some additional vertical space

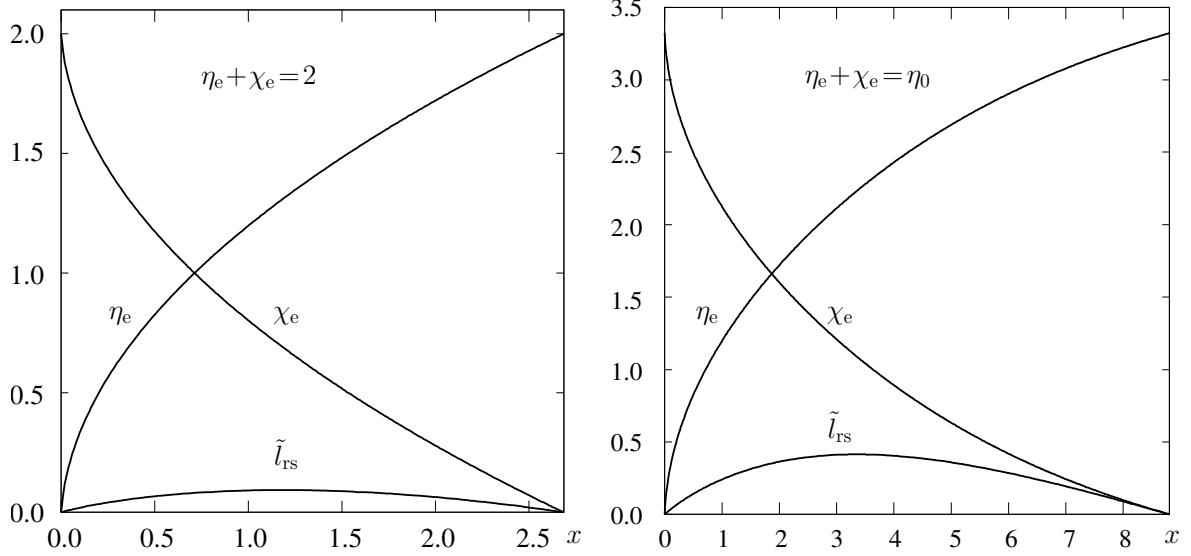


Figure 4. The paths of photons with arrival time at epochs: $\eta = 2$ (left) and $\eta_0 = 3.3224$ (right).

space

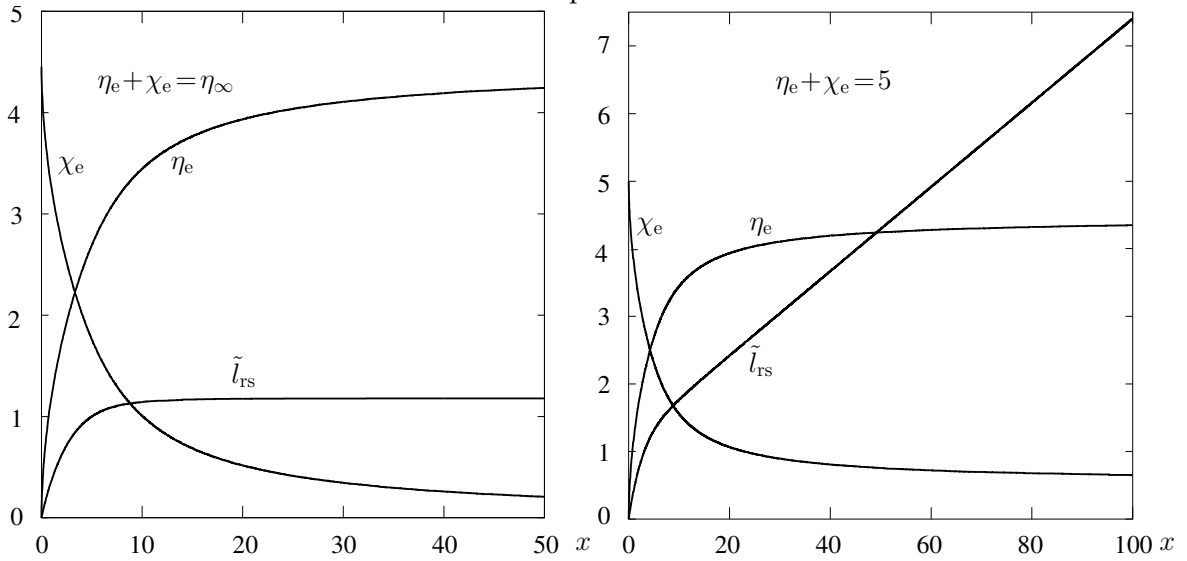


Figure 5. The paths of photons with "arrival" time at epochs: $\eta_\infty = 4.4514$ (left) and $\eta = 5$ (right).

436 the distant past, when neither the Earth, nor even the Sun, existed (but the galaxies and stars of the
437 previous generations had already formed).

438 Figure 4 shows that the distance of a photon emitted sufficiently early at first increases, which
439 means expansion with a speed greater than the speed of light, faster than the photon speed. From the
440 point where the distance reaches a maximum, the photon begins to approach and finally arrives at our
441 location. However, as shown in Figure 5, this is not possible if $\eta_e + \chi_e \geq \eta_\infty$, even if the equality is true.
442 Figure 5 left shows that a photon emitted at the second horizon, and which then travels along it, would
443 not arrive at the observer after an infinite time; in fact, the photon only recedes along with the horizon.
444 After an infinite time, such a photon will be at a distance $l_\Lambda \approx 5.0$ Gpc, since the factor $\eta_\infty - \eta$ in the
445 formula (63) at $\chi_e + \eta_e = \eta_\infty$ tends to zero if $t \rightarrow \infty$, while the factor $a(\eta) \rightarrow \infty$, but their product
446 remains finite. A photon emitted at $\eta_e + \chi_e < \eta_\infty$ may, after a very long time, reach the current location
447 of our civilization, but one emitted at $\eta_e + \chi_e > \eta_\infty$ will only recede from us, eventually exponentially
448 fast. The reason for this is the accelerated expansion of space. Thus, galaxies located on the second
449 horizon and behind it will forever disappear from our field of view. These statements follow from the
450 formulas given below.

451 5.2. Distances, velocities, and accelerations of horizons

452 Distances to horizons at an arbitrary epoch η according to equations (64) are defined by the
453 formulas:

$$l_{\text{GHor}} = l_{\text{H}}^0 a(\eta) \eta = l_\Lambda x I_0(x, \beta), \quad (65)$$

$$l_{\text{KHor}} = l_{\text{H}}^0 a(\eta) (\eta_\infty - \eta) = l_\Lambda x [I_0(\infty, \beta) - I_0(x, \beta)]. \quad (66)$$

454 The sum of the horizon conformal space coordinates is constant at all times, and the sum of the
455 distances to them is proportional to the scale factor. Both horizons expand. The speed of the geometric
456 horizon exceeds by the speed of light the velocity of the position where the horizon is located at time
457 $\dot{l}_{\text{GHor}} = l_{\text{H}}^0 \dot{a} \eta + l_{\text{H}}^0 a \dot{\eta} = H l_{\text{GHor}} + c$. It expands at an accelerating rate. In contrast, the velocity of the
458 kinematic horizon is less than the speed of its location by the speed of light: $\dot{l}_{\text{KHor}} = l_{\text{H}}^0 \dot{a} (\eta_\infty - \eta) -$
459 $l_{\text{H}}^0 a \dot{\eta} = H l_{\text{KHor}} - c$, and its expansion slows down.

460 Asymptotes of distances to horizons and their velocities at $t \rightarrow \infty$, $a \rightarrow \infty$, $z \rightarrow -1$ are determined
461 by taking into consideration that $I_0(\infty, \beta) = 0.42880$ and $I_0(\infty, \beta) - I_0(x, \beta) \sim \frac{1}{x} \left(1 - \frac{1}{8} \frac{\beta}{x^3}\right)$:

$$l_{\text{GHor}} \sim l_{\text{H}}^0 \eta_* I_0(\infty, \beta) a = 5.9 \cdot 10^{28} a \text{ cm} \sim 2.7 \cdot 10^{28} e^{H\Lambda t} \text{ cm} \rightarrow \infty, \quad (67)$$

$$l_{\text{KHor}} \rightarrow \frac{c}{H_\Lambda} = 1.56 \cdot 10^{28} \text{ cm} = 5.05 \text{ Gpc}. \quad (68)$$

462 The current distance to the geometric horizon is $l_{\text{GHor}}^0 = l_{\text{H}}^0 \eta_0 = 3.32 l_{\text{H}}^0 = 4.39 \cdot 10^{28} \text{ cm} = 14.2$ Gpc.
463 The velocity near the horizon is $v_{\text{GHor}}^0 = c \eta_0 = 3.32c$, and the velocity of the expansion of the horizon
464 is $\dot{l}_{\text{GHor}}^0 = 4.32c$. The horizon will cross 4.32 light years in one year, which is equal to 1.33 pc, so that
465 1 Gpc will be added to the current 14.2 Gpc in $0.755 \cdot 10^9$ years if the speed of the horizon is equal to its
466 current velocity, and in $0.741 \cdot 10^9$ years if the increase of the velocity is taken into account.

467 The current distance to the second horizon is $l_{\text{KHor}}^0 = l_{\text{H}}^0 (\eta_\infty - \eta_0) = 1.49 \cdot 10^{28} \text{ cm} = 4.84$ Gpc. The
468 limit to this distance coincides with the Hubble limit: $l_{\text{KHor}} \rightarrow \frac{l_{\text{H}}^0}{\sqrt{\Omega_\Lambda^0}} = \frac{c}{H_\Lambda} = 5.05$ Gpc. The current
469 speed of expansion of the location of this horizon is $c(\eta_\infty - \eta_0) = 1.13c$, and the speed of recession of
470 the kinematic horizon from us is now $0.13c$.

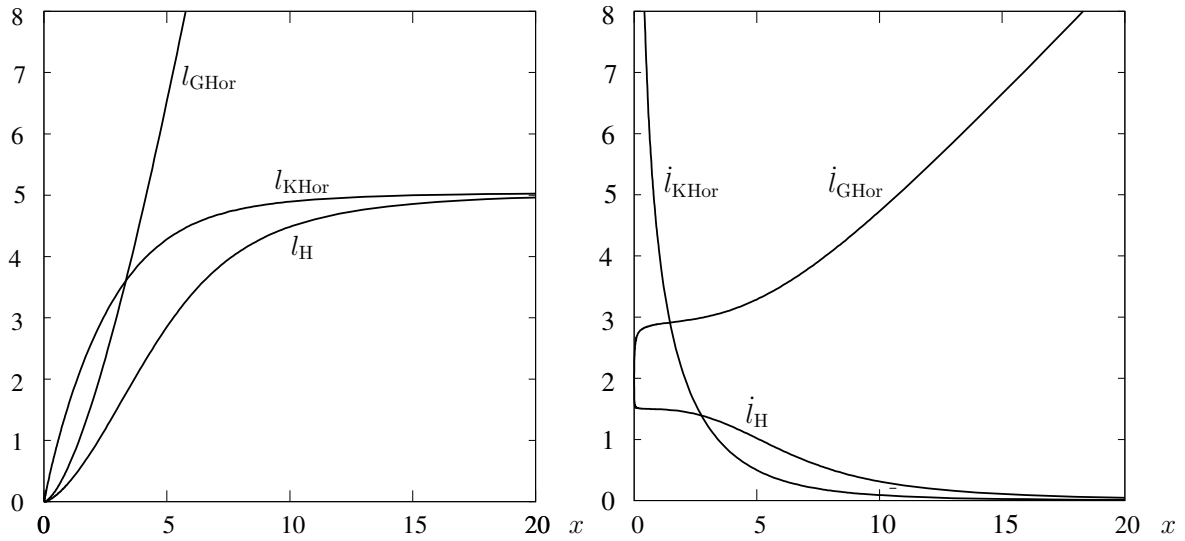


Figure 6. Left: Hubble distance and distances to the horizons in Gpc. Right: Speeds of change of distances in units of the speed of light. (right).

471 The velocities of the horizons at an arbitrary moment and their asymptotics for $t \rightarrow \infty$ and
 472 $x \sim 5.0 \cdot e^{H_\Lambda t} \rightarrow \infty$ are

$$\dot{l}_{\text{GHor}} = l_{\text{H}}^0 (\dot{a}\eta + a\dot{\eta}) = H l_{\text{GHor}} + c = c \left[\frac{\sqrt{1 + \beta x + x^4}}{x} I_0(x, \beta) + 1 \right] \sim c x I_0(\infty, \beta), \quad (69)$$

$$\dot{l}_{\text{KHor}} = c \left[\frac{\sqrt{1 + \beta x + x^4}}{x} [I_0(\infty, \beta) - I_0(x, \beta)] - 1 \right] \sim \frac{3}{8} \frac{\beta}{x^3} c. \quad (70)$$

473 It is interesting to note that all points with fixed coordinate χ begin (at the initial instant of the
 474 expansion) to move away from each other at an infinite speed (according to (37), $\dot{a} = \dot{x}/x_0 =$
 475 $(H_\Lambda/x_0)\sqrt{1 + \beta x + x^4}/x$). The geometric horizon begins to expand with velocity $2c$, as does the
 476 Hubble distance, but the evolution of their velocities is opposite (see formulas (53) and (67)). For small
 477 x , the velocity \dot{l}_{GHor} grows very fast, while the velocity \dot{l}_{H} rapidly decreases, so that at $x = 0.03$ they
 478 become equal to $2.50c$ and $1.56c$, respectively. The second horizon begins the expansion, as do all
 479 ordinary points of space, with an infinite speed, which decreases very rapidly.

480 Accelerations have similar evolution:

$$\begin{aligned} \ddot{l}_{\text{GHor}} &= l_{\text{H}}^0 (\ddot{a}\eta + 2\dot{a}\dot{\eta} + a\ddot{\eta}) = \frac{\ddot{a}}{a} l_{\text{GHor}} + l_{\text{H}}^0 \left(2\dot{a} \frac{H_0}{a} - a \frac{H_0}{a^2} \dot{a} \right) = -\frac{4\pi G}{3} \rho_{\text{g}} l_{\text{GHor}} + cH = \\ &= cH_\Lambda \left[\frac{\sqrt{1 + \beta x + x^4}}{x^2} + \frac{x^4 - \beta x/2 - 1}{x^3} I_0(x, \beta) \right] \sim cH_\Lambda I_0(\infty, \beta) x, \end{aligned} \quad (71)$$

$$\begin{aligned} \ddot{l}_{\text{KHor}} &= l_{\text{H}}^0 [\ddot{a}(\eta_\infty - \eta) - 2\dot{a}\dot{\eta} - a\ddot{\eta}] = \frac{\ddot{a}}{a} l_{\text{KHor}} - l_{\text{H}}^0 \left(2\dot{a} \frac{H_0}{a} - a \frac{H_0}{a^2} \dot{a} \right) = \\ &= -\frac{4\pi G}{3} \rho_{\text{g}} l_{\text{H}}^0 \frac{x}{x_0} \frac{I_0(\infty, \beta) - I_0(x, \beta)}{(\Omega_{\text{r}}^0 \Omega_{\Lambda}^0)^{1/4}} - cH = \\ &= cH_\Lambda \left[\frac{x^4 - \beta x/2 - 1}{x^3} [I_0(\infty, \beta) - I_0(x, \beta)] - \frac{\sqrt{1 + \beta x + x^4}}{x^2} \right] \sim -\frac{9}{8} \frac{\beta}{x^3} cH_\Lambda. \end{aligned} \quad (72)$$

481 At $x = x_0$, we obtain the current values of the velocities (see above) and accelerations: $\dot{l}_{\text{GHor}}^0 =$
 482 $3.45 H_\Lambda c = 19.9 \cdot 10^{-8} \text{ cm/s}^2$, $\dot{l}_{\text{KHor}}^0 = -1.95 H_\Lambda c = -11.3 \cdot 10^{-8} \text{ cm/s}^2$.

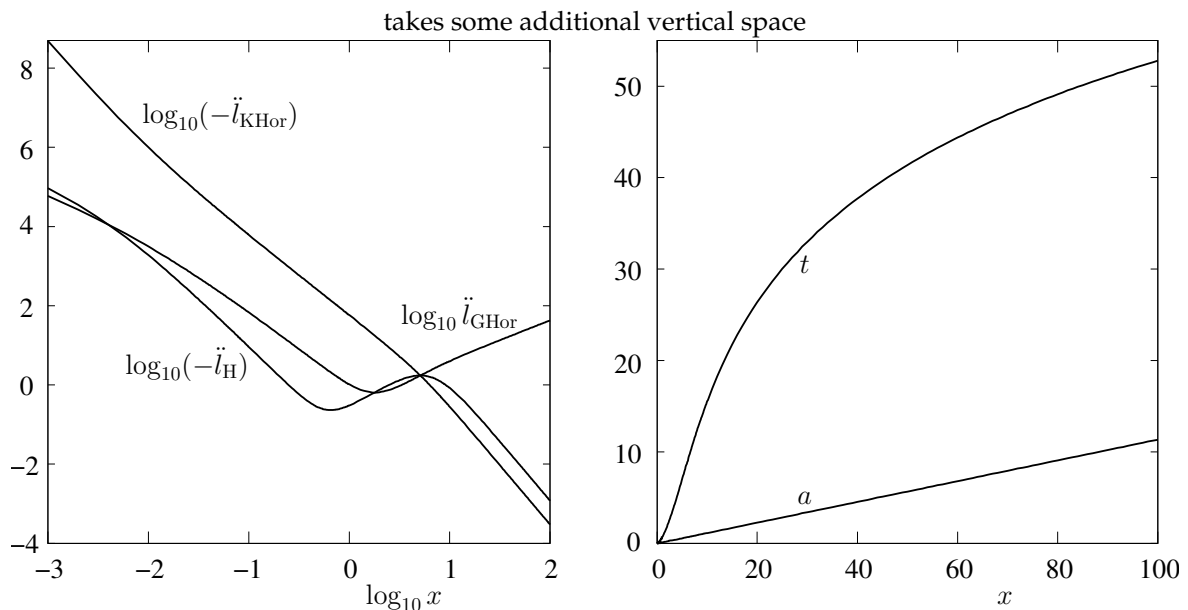


Figure 7. *Left:* Accelerations of the horizons and the Hubble distance. *Right:* Values of a and t as functions of x .

483 The speed of the first horizon increases, while that of the second horizon decreases. During the
 484 entire period of action of the cosmological acceleration ($6.5 \cdot 10^9$ years), the velocity of the first horizon
 485 increased from $3.31 c$ (by the value of η for $\rho_g = 0$ in Table 1) to the current velocity of $4.32 c$, and the
 486 speed of the second horizon decreased from $0.479 c$ to $0.129 c$.

487 Figure 6, *left* presents the distances to the horizons, and Figure 6, *right* shows their velocities as a
 488 function of the parameter x . The figures give the same values for the Hubble distance. All distances are
 489 given in Gpc, and velocities are indicated in units of the speed of light. At first, until $\eta_\infty - \eta > \eta$, the
 490 distance to the second horizon is greater than that to the first horizon. The horizons intersected when
 491 $\eta_{\text{crs}} = \eta_\infty / 2 = 2.23$, $x_{\text{crs}} = 4.08$, $z_{\text{crs}} = 1.677$ at an epoch $t_{\text{crs}} = 3.93$ billion years from the beginning,
 492 that is $t_0 - t_{\text{crs}} = 9.80$ billion years ago (earlier than the acceleration began), when the distance to
 493 the horizons was 3.58 Gpc. Prior to this, the first horizon determined the initial possibility to make
 494 observations (if there were observers at that time). Since then, the second horizon has become closer.
 495 Note, however, that the horizon effects differ. The first horizon (in fact, not it, but the physical horizon)
 496 limits the spherical region of space in which one can observe the past history of the universe, while the
 497 second defines those areas of information that will never reach the observer.

498 Figure 7, *left* plots the accelerations of the horizons and Hubble distance, measured in units of
 499 cH_Λ , on a logarithmic scale. Only the acceleration of the second horizon is a monotonic function; \ddot{l}_{GHor}
 500 has a minimum, while \ddot{l}_{H} has both a minimum and a maximum. The figures show a linear increase
 501 of the acceleration \ddot{l}_{GHor} with x , and the equality of the rates of decrease of the accelerations \ddot{l}_{H} and \ddot{l}
 502 according to the asymptotes (55) and (72). Figure 7, *right* shows the relationship of the scale factor a
 503 and cosmological time t with the parameter x .

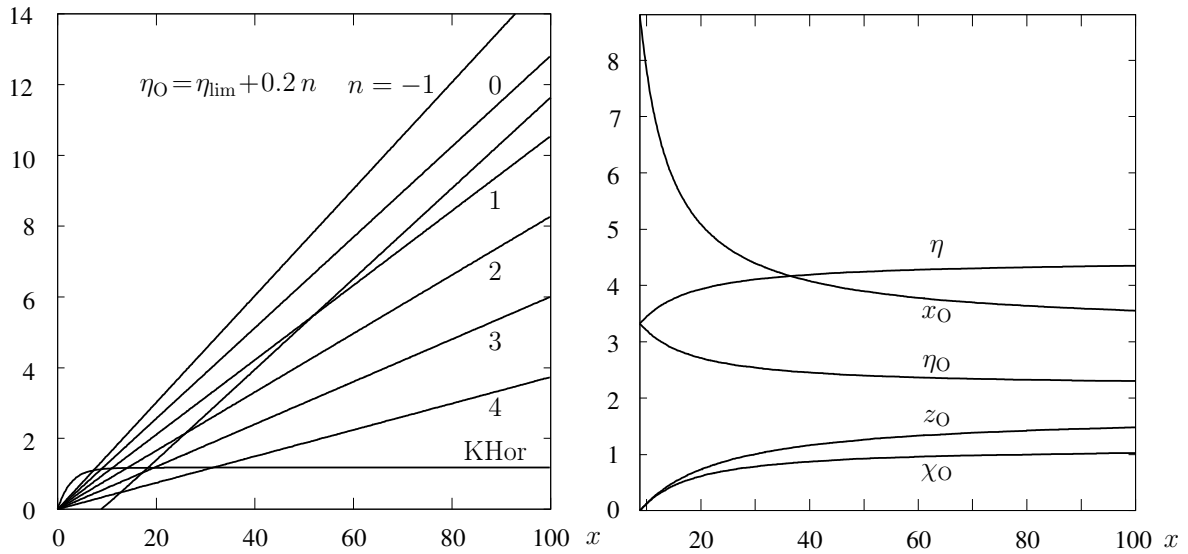
504 5.3. Connection with extraterrestrial civilizations

Suppose that at the current epoch ($t = t_0$, $\eta = \eta_0$) humans emit a radio signal in some direction. The distance to it increases; for a value of the time coordinate η the distance will be equal to $l_{\text{ph}} = l_{\text{H}}^0 a(\eta)(\eta - \eta_0)$, $\eta \geq \eta_0$. Its speed includes both the speed of expansion and the speed of light:

$$\dot{l}_{\text{ph}} = l_{\text{H}}^0 \dot{a}(\eta - \eta_0) + l_{\text{H}}^0 a \dot{\eta} = H l_{\text{ph}} + c. \quad (73)$$

Table 5. Objects along the signal path.

η_O	x_O	a_O	z_O	l_O^0 Gps	t_O
1.99	2.67	0.303	2.30	5.69	2.89
2.19	3.23	0.367	1.73	4.84	3.83
2.39	3.87	0.440	1.28	3.98	4.95
2.59	4.60	0.523	0.913	3.12	6.29
2.79	5.46	0.620	0.613	2.27	7.88
2.99	6.49	0.737	0.357	1.41	9.77

**Figure 8.** *Left:* Path of the signal to objects. *Right:* Objects reachable by the signal.

505 For brevity, we omit the factor l_H^0 , which means that we use distances measured in units of the modern
 506 Hubble distance. On the way, the signal passes by objects with fixed spatial coordinates $\chi_O = \eta_0 - \eta_O$.
 507 Distances to these objects grow only due to the cosmological expansion, that is, increasing scale
 508 factor: $\tilde{l}_O = a(\eta)(\eta_0 - \eta_O)$. The signal catches up with these objects when their distances from us
 509 become equal, which occurs at the moment η_{mt} , when $\eta_{mt} - \eta_0 = \eta_0 - \eta_O$, $\eta_{mt} = 2\eta_0 - \eta_O$; therefore,
 510 $\tilde{l}_{ph} = \tilde{l}_O = a(2\eta_0 - \eta_O)(\eta_0 - \eta_O)$. Since η_{mt} cannot exceed η_∞ , the signal can meet for a finite (although,
 511 perhaps, very large) time only those objects whose coordinate satisfies $\chi_O < \eta_\infty - \eta_0 = 1.13$. This
 512 implies that the coordinate has the same boundary as a photon traveling toward us. This boundary is
 513 the second horizon (see above), and $\eta_O > \eta_{lim} = 2\eta_0 - \eta_\infty = 2.19$.

Figure 8, *left* contains lines that plot the dependence of the distance l_O on the coordinate x up to six objects. Positions of the signal path and the kinematic horizon are indicated as well. The objects are characterized by values of $\eta_O = \eta_{lim} + 0.2n$, $n = -1(1)4$. The corresponding values of x_O , the scale factor $a_O = a(\eta_O)$, and the redshift z_O , as well as the current distances to these objects l_O^0 , are given in Table 5. It can be seen from the figure that the emitted signal reaches the objects only when $n = 1, 2, 3, 4$. The signal comes earlier to objects with larger values of η_O , and hence smaller values of z_O and l_O . These objects are located closer to the position of the signal output at the moment of its emission. The signal only catches up to objects with $n = 3$ and 4, for which the values of η_O are equal to 2.79 and 2.99, respectively, before they cross the second horizon. The condition of this is $\eta_0 - \eta_O < \eta_\infty - 2\eta_0 + \eta_O$, that is, $\eta_O > \eta_h = \frac{3\eta_0 - \eta_\infty}{2} = 2.758$. The distance between the object,

which is now almost on the second horizon (the current distance to it is 4.84 Gpc and its redshift is 1.72), and the signal for $\tilde{l}_O^0 = \eta_\infty - \eta_0 - \varepsilon$, $\eta_O = \eta_{\text{lim}} + \varepsilon$ is

$$l_O - l_{\text{ph}} = l_{\text{H}}^0 a(\eta)(\eta_0 - \eta_{\text{lim}} - \varepsilon) - l_{\text{H}}^0 a(\eta)(\eta - \eta_0) = l_{\text{H}}^0 a(\eta)(\eta_\infty - \varepsilon - \eta) \sim \frac{c}{H_\Lambda} \frac{\eta_\infty - \varepsilon - \eta}{\eta_\infty - \eta}, \quad (74)$$

514 since, according to eqs. (38) and (41), $\eta \sim \eta_\infty - \eta_*/x$, $a(\eta) = x/x_0 \sim 1/\left[\sqrt{\Omega_\Lambda^0}(\eta_\infty - \eta)\right]$ for $x \rightarrow \infty$,
 515 $\eta_\infty - \eta \ll 1$. The difference (74) tends to zero for $\eta \rightarrow \eta_\infty - \varepsilon$ if $\varepsilon > 0$. Thus, in agreement with Figure 8,
 516 left, the signal will still reach a given object if the object is located at least slightly closer than the second
 517 horizon. The time that the signal needs to meet the object is $t \sim \ln(1/\varepsilon)$. If the object is located on the
 518 horizon ($\varepsilon = 0$), there remains an insurmountable distance $c/H_\Lambda = 5.05$ Gpc. The distance between
 519 the signal emitted now and objects currently located behind the second horizon will only increase with
 520 time. In addition, it will increase asymptotically as an exponential function. These objects are carried
 521 away by the exponential expansion, that is, by the repulsion of the dark energy. In models without
 522 repulsion the second horizon does not appear.

Figure 8, right shows the dependences of the coordinates x_O , η_O and $\chi_O = \eta_0 - \eta_O$, as well as redshifts z_O of objects that the signal will reach at the time corresponding to its coordinate x . The figure plots also the dependence of the time coordinate η on x . The signal emitted now will reach the second horizon when

$$l_{\text{ph}} = l_{\text{H}}^0 a(\eta_{\text{h}})(\eta_{\text{h}} - \eta_0) = l_{\text{KHor}} = l_{\text{H}}^0 a(\eta_{\text{h}})(\eta_\infty - \eta_{\text{h}}), \quad \eta_{\text{h}} = \frac{\eta_0 + \eta_\infty}{2} = 3.89. \quad (75)$$

523 The corresponding values are $x_{\text{h}} = 18.3$, $l_{\text{ph}} = l_{\text{KHor}} = 5.02$ Gpc, and $t_{\text{h}} = 24.9$ Gyr. At this time
 524 an object with initial coordinate $x_O = 5.30$ will approach the horizon. This coordinate corresponds
 525 to $a_O = 0.601$, $z_O = 0.663$, and an initial distance to us of $l_O^0 = l_{\text{H}}^0(\eta_0 - \eta_O) = 1.45$ Gpc, because if
 526 $l_O = l_{\text{ph}} = l_{\text{KHor}}$ then $\eta_0 - \eta_O = \eta_{\text{h}} - \eta_0 = \eta_\infty - \eta_{\text{h}}$ and $\eta_O = (3\eta_0 - \eta_\infty)/2 = 2.76$.

527 The signal sent by us can reach distances only up to ≈ 5 Gpc to have any hope to get a reply.
 528 Exponential expansion of space entrains radiation both going away from us and directed toward us.
 529 Nevertheless, 5 Gpc is a very large distance, and inside the sphere of such a radius there are many
 530 galaxies. If the signal hits a planet populated by intelligent creatures who have reached an advanced
 531 stage of civilization, they can receive it, understand, determine the direction from what it came, and
 532 reply. Then their signal will approach that place where humans were when we sent the first signal.
 533 The distance of their signal to us will change according to the formula $\tilde{l}_{\text{ret}} = a(\eta)(\eta_{\text{mt}} - \eta_0 - \eta) =$
 534 $a(\eta)(\eta_0 - \eta_O - \eta) = a(\eta)(3\eta_0 - 2\eta_O - \eta)$. Any reply will arrive at Earth at time $\eta_{\text{ret}} = 3\eta_0 - 2\eta_O$.
 535 If we want a reply to arrive at time η_{ret}^0 , $\eta_0 < \eta_{\text{ret}}^0 < \eta_\infty$, then such a civilization should have
 536 $\eta_O > (3\eta_0 - \eta_{\text{ret}}^0)/2$ and $\chi_O < (\eta_{\text{ret}}^0 - \eta_0)/2$. In an extreme case, if we assume that $\eta_{\text{ret}}^0 = \eta_\infty$,
 537 then the condition $\eta_{\text{ret}} < \eta_\infty$ imposes a restriction on the coordinate η_O : $\eta_O > (3\eta_0 - \eta_\infty)/2$. This
 538 restriction coincides with the condition that the signal reaches the object (civilization) before the
 539 latter reaches the second horizon. The restriction on the spatial coordinate is as it was previously:
 540 $\chi_O = \eta_0 - \eta_O < (\eta_\infty - \eta_0)/2$.

541 It is clear that it makes sense to send a signal to objects located closer than several dozen light
 542 years, otherwise any possible reply would take too long. Undoubtedly, it will be necessary to limit the
 543 search within our Galaxy and even the immediate vicinity of the solar system. Even in this case the
 544 signals must either be sent in a very narrow cone, or they should be sufficiently energetic so that they
 545 can be received at a greater distance.

546 Although the above arguments have a purely theoretical or even academic character, they establish
 547 restrictions on the limits imposed by the model. They can be related either to epochs when our
 548 civilization on the Earth has not existed yet, or has not been able to realize connections with other
 549 civilizations, or to the epochs when the Sun and Earth will no longer exist in their current form.

550 However, these same arguments apply to any arbitrary location in the universe and to civilizations
551 that may arise and prosper at any time.

552 6. Conclusion

553 In this paper we have summarized results of the Standard model that reveal some of its
554 quantitative properties. After a brief excursion into the history of creation of cosmological models,
555 we have presented the two Friedmann-Lemaître equations, which describe a uniform and isotropic
556 universe, and have restated the definitions of the critical values and five cosmological distances. Based
557 on the compatibility condition of two equations and on the equations of state, we have derived the
558 laws of the change with time of the mass density of four noninteracting components: the density of
559 matter decreases as the third order of the scale factor and the density of radiation and neutrinos as
560 the fourth order, while the dark energy density is unchanged. These laws provide solutions of the
561 cosmological equations in quadratures.

562 The equations are specified for the flat space-time model. Using the parameters of this model
563 obtained from observations: Hubble constant, $H_0 = 70$ km/s/Mpc, temperature of the cosmic
564 background radiation, $T_0 = 2.7727$ K, dark energy fraction of the total cosmological mass density,
565 $\Omega_\Lambda^0 = 0.72$, we have determined the current Hubble distance $l_H^0 = 4.28$ Gpc, the critical density
566 $\rho_c = 9.2 \cdot 10^{-30}$ g/cm³, and the fractional contributions to ρ_c of the radiation, $5 \cdot 10^{-5}$, six types
567 of neutrinos $6.9 \cdot 10^{-5}$, and dust-like matter, ≈ 0.28 , which includes dark matter. They define the
568 relationships of the scale factor $a = 1/(1+z)$ (and, thus, of the redshift z), the conformal dimensionless
569 time coordinate η , and the dimensionless parameter x with cosmological time t . For the early and late
570 stages of expansion, simple and sufficiently accurate approximations of these relationships have been
571 obtained. We have shown that, in contrast to redshift, coordinates η and x are not tied to a specific
572 epoch of evolution. Several dimensionless parameters of the model have been introduced that are also
573 free from such binding, and their quantitative values have been derived.

574 It has been shown that major events in the evolution of the universe occurred near the beginning,
575 when the dominant carrier of the mass density transferred from radiation and neutrinos to “dust” —
576 corresponding to z changing from 5500 to 1000 — and then later when dark energy became dominant,
577 at $z = 0.7$ to 0.4.

578 Dependencies of different types of distances have been calculated as functions of parameters x
579 and z , as well as speeds of their changes. A difference between the cosmological redshift and classical
580 Doppler effect was stressed, which was explained by the fact that a shift of the frequency of a photon
581 occurs not only at the time of its emitting by a cosmical object, but at every point of its path to the
582 observer.

583 We have discussed the concepts of two horizons: geometric, inherent in any expanding model,
584 and kinematic, typical for models expanding with an acceleration. Distances to these horizons, along
585 with speeds and accelerations of evolution of these distances, have been derived as functions of time.
586 Current distances to the horizons are 14.2 Gpc for the first horizon and 4.84 Gpc to the second horizon.
587 The horizons crossed each other 9.8 Gyr ago, when the distance to them was 3.58 Gpc.

588 The current acceleration of expanding space represents the most surprising value: at the Hubble
589 distance, where the expansion rate is equal to the speed of light, the acceleration is about $4 A/s^2$. Such
590 a value of the acceleration has been reached over the past 6.5 billion years, while it was zero at the
591 beginning of the expansion. A limit on the acceleration for $t \rightarrow \infty$ at the limit of the Hubble distance is
592 $5.7 A/s^2$. Even at the current horizon the acceleration is only slightly higher, $\approx 20 A/s^2$. However, tens
593 of billions of years into the future, the acceleration of the horizon and scale factor (indeed, all scales)
594 will increase over time exponentially with an exponent of t/t_Λ , where $t_\Lambda = 16.5$ Gyrs. This means that
595 a second inflation will occur.

596 We have estimated the rate of change of redshifts and apparent luminosities of objects with
597 increasing age of the universe. For distant objects with $z > 13.2$, the apparent luminosity can grow

598 with time. However, detection of these effects requires very long time intervals between observations,
599 as well as significant improvements in the capabilities of observational instruments in the future.

600 We have estimated distances across which our signal emitted from the Earth can reach
601 extraterrestrial civilizations and from which they can respond to us. These distances are quite large, on
602 the order of 5 Gpc, so that they do not limit the possibilities of contact with other civilizations in the
603 universe.

604 The above discussion provides a quantitative description of various geometric and kinematic
605 properties of the Standard model that is currently considered to be an accurate description of
606 the universe. Future observationally driven revisions of the cosmological parameters such as the
607 Hubble constant would require updates to the exact values of the parameters that we have derived.
608 Nevertheless, as long as the cosmological constant dominates the current and future energy of the
609 universe, seemingly odd features, such as the presence of two horizons, will remain intact.

610 **Acknowledgments:** SJ acknowledges partial support from Russian Science Foundation grant 17-12-01029.

611 **Author Contributions:** DN and SJ contributed 70% and 30%, respectively, to this work.

612 **Conflicts of Interest:** The authors declare no conflict of interest.

613 References

- 614 1. Zeldovich, Ya.B.; Novikov, I.D. 1975. *The Structure and Evolution of the Universe*. University of Chicago
615 Press, Chicago. **1983**.
- 616 2. Narlikar, J.V. *Introduction to Cosmology*. Cambridge, Cambridge University Press. **1993**.
- 617 3. Misner, T.W.; Thorn, K.S.; Wheeler, J.A. *Gravitation*. San Francisco, Freeman. **1972**.
- 618 4. Weinberg, S. *Gravitation and Cosmology: Principles and Applications of the General Theory of Relativity*.
619 New York, John Wiley and Sons, Inc. **1972**.
- 620 5. Gorbunov, D.C.; Rubakov, V.A. *Introduction to the Theory of the Early Universe. The Theory of Hot Big Bang*.
621 M., URSS. **2008**.
- 622 6. Einstein, A. Die Grundlage der allgemeine Relativitätstheorie. *Ann. d. Phys.* **1916**, *49*, 760.
- 623 7. Einstein, A. Kosmologische Betrachtungen zur allgemeinen Relativitätstheorie. *Sitzungsberichte der Preuss.*
624 *Acad. Wiss.* **1917**, 142–152. (English translation: H.A.Lorents, A.Einstein, H.Minkowski, H.Weil. **1950**. *The*
625 *principle of relativity*. 177–188. Methuen, London.)
- 626 8. Eddington, A. *The Mathematical Theory of Relativity*. Second edition. Cambridge. At the University Press.
627 **1924**.
- 628 9. de Sitter, W. On Einstein's theory of gravitation and its astronomical consequences, Third paper. *Monthly*
629 *Notices Roy. Astron. Soc.* **1917**, *78*, 3–28.
- 630 10. Friedmann, A. Über die Krümmung des Raumes. *Zeitschrifts für Physik.* **1922**, *10*, 377–386.
- 631 11. Friedmann, A. Über die Möglichkeit einer Welt mit konstanter negativer Krümmung des Raumes. *Zeitschrifts*
632 *für Physik*, **1924**, *21*, 326.
- 633 12. Lemaître, G. Un universe homogène de masse constante et de rayon croissante rendant compte de la
634 vitesse radiale des nébuleuses extragalactiques. *Annales de la Société scientifique de Bruxelles.* **1927**, *47 A*,
635 41. A homogeneous universe of constant mass and increasing radius accounting for the radial velocity of
636 extra-galactic nebulae. *Mon. Not. R. Astron. Soc.* **1931**, *91*, 483–490.
- 637 13. Lemaître, G. The expanding universe. *Mon. Not. R. Astron. Soc.* **1931**, *91*, 490–501.
- 638 14. Einstein, A. Grundgedanken und Probleme der Relativitätstheorie. In "Nobelstiftelsen, Les Prix Nobel en
639 1921–1922". Imprimerie Royal, Stockholm. **1923**.
- 640 15. Einstein, A. Zum kosmologischen Problem der allgemeinen Relativitätstheorie. *Sitzungsber. Preuss. Acad.*
641 *Wiss., phys.-math. Kl.*, **1931**, 235–237.
- 642 16. Hubble, E. A relation between distance and radial velocity among extragalactic nebulae. *Proc. Nat. Acad. Sci.*
643 *USA*, **1929**, *15*, 168.
- 644 17. Sandage, A. Observational tests of world models. *Ann. Rev. Astron. Astrophys.* **1988**, *26*, 561–630.
- 645 18. Sandage, A. Current problems in the extragalactic distance scale. *Astrophys. J.* **1958**, *127*, 513–527.
- 646 19. Sandage, A.; Tammann, G.A. Steps towards the Hubble constant. VIII. The global value. *Astrophys. J.* **1982**,
647 *256*, 339–345.

- 648 20. Sandage, A. The redshift-distance relation. II. The Hubble diagram and its scatter for first-ranked cluster
649 galaxies: a formal value for q_0 . *Astrophys. J.* **1972**, *178*, 1–24.
- 650 21. Hoyle, F.; Burbidge, G.; Narlikar, J.V. *A Different Approach to Cosmology. From a static universe through the*
651 *big bang towards reality.* Cambridge University Press. **2000**.
- 652 22. Frieman, J.A.; Turner, M.S.; Huterer, D. Dark energy and accelerating universe. *Annu. Rev. Astron. Astrophys.*
653 **2008**, *46*, 385–432.
- 654 23. Gliner, E.B. Algebraic properties of the energy-momentum tensor and vacuum-like states of matter. *Zhurn.*
655 *Experim. Theor. Fizik.* **1965**, *49*, 542–548.
- 656 24. Guth, A. Inflationary universe: a possible solution to the horizon and flatness problems. *Phys. Rev. D.* **1981**,
657 *23*, 347–356.
- 658 25. Linde, A.D. *The physics of elementary particles and inflationary cosmology.* M. Nauka. **1990**.
- 659 26. Riess, A.S.; et al. Observational evidence from supernovae for an accelerating universe and a cosmological
660 constant. *Astron. J.* **1998**, *116*, 1009–1038.
- 661 27. Perlmutter, S.; et al. Measurements of Ω and Λ from 42 high-redshift supernovae. *Astrophys. J.* **1999**, *517*,
662 565–586.
- 663 28. Knop, R.A.; Aldering, G.; Amanullah, R.; Astier, P.; Blanc, G.; et al. New constraints on Ω_M , Ω_Λ , and w from
664 an independent set of 11 high-redshift supernovae observed with the Hubble Space Telescope. *Astrophys. J.*
665 **2003**, *598*, 102–137.
- 666 29. Hinshaw, G.; Larson, D.; Komatsu, E.; et al. Nine-year Wilkinson Microwave Anisotropy Probe (WMAP)
667 observations: cosmological parameters results. *Astrophys. J. Suppl. Series.* **2013**, *208*, 19.
- 668 30. DES Collaboration: Abbott, T.M.C.; Allam, S.; Andersen, P.; et al. First Cosmology Results
669 using Type Ia Supernovae from the Dark Energy Survey: Constraints on Cosmological Parameters.
670 arXiv:astro-ph/1811.02374.
- 671 31. Macaulay, E. R.; Nichol, C.; Bacon, D.; et al. DES Collaboration. First Cosmological Results using Type Ia
672 Supernovae from the Dark Energy Survey: Measurement of the Hubble Constant. arXiv:astro-ph/1811.02376.
- 673 32. Nagirner, D. I.; Turichina, D. G. The effect of neutrino mass in cosmology. *Astrophysics*, **2019**, *62*, 108–128.
- 674 33. McCrea, W.H. Observable relations in relativistic cosmology. *Zeitschrift für Astrophysik.* **1935**, *9*, 290–314.
- 675 34. Harrison, E. The redshift-distance and velocity-distance laws. *Astrophys. J.* **1993**, *403*, 28–31.
- 676 35. Alpher, R.; Herman, R. The Origin and Abundance Distribution of the Elements. *Ann. Rev. Nucl. Astropart.*
677 *Sci.* **1953**, *2*, 1–40.
- 678 36. Sandage, A. The change of redshift and apparent luminosity of galaxies due to the deceleration of selected
679 expanding universes. *Astrophys. J.* **1962**, *136*, 319–333.
- 680 37. McVittie, G.C. Appendix. *Astrophys. J.* **1962**, *136*, 334–338.
- 681 38. Loeb, A. Direct measurement of cosmological parameters from the cosmic deceleration of extragalactic objects.
682 *Astrophys. J.* **1998**, *499*, L111–L114.
- 683 39. Liske, J.; et al. Cosmic dynamics in the era of Extremely Large Telescopes. *Mon. Not. R. Astron. Soc.* **2008**,
684 *386*, 1192–1218.
- 685 40. Rindler, W. Visual horizons in world-models. *Mon. Not. R. Astron. Soc.* **1956**, *116*, 662–677.
- 686 41. Margalef-Bentabol, B.; Margalef-Bentabol, J.; Cepa, J. Evolution of the cosmological horizons in a universe
687 with countably infinitely many state equations. *Journal of Cosmology and Astroparticle Physics.* **2013**. 015.
688 arXiv:astro-ph/1302.2186.